Chapter 4
Physical Fields and Modeling

Cybernetical systems are natural systems with complex phenomena in a multi-dimensional environment. The concept of a physical field is given here as a three-dimensional field of (x, y, z), where x, y are considered a surface coordinates and z, a space coordinate. Our main task is to identify a system in a physical field using our knowledge of certain variables and considering their interactions in the environment and with physical laws. Researchers are experimenting to predict the behavior of various complex systems by analyzing emperical data using advanced techniques. Resulting mathematical models must be able to extrapolate the behavior of complex systems in (x,y) coordinates, as well as predict in time t another dimension in the coordinate system. The possibility of better modeling is related through the use of heuristic methods based on sorting of models, pretendents in the form of finite difference equations, empirical data, and selection criteria developed for that purpose.

Examples of physical fields may be fields of air pollution, water pollution, meteorological systems and so on. Observations of various variables—such as data about distributed space, intensity, and period of variable movement—are used for identifying such fields. It corresponds to the observations from control stations corresponding to input and output arguments. The problem goal may be interpolation, extrapolation or prediction, where the area of interpolation lies within the multi-bounded area, and the area of extrapolation or prediction lies outside the area of interpolation process. Models must correspond to the future course of processes in the area. Problems Can be further extended to short-range, long-range or combined forecasting problems depending on principles and selection of arguments. A model must correspond to the function (or solution of differential equation) that has the best agreement with future process development. A physical model can be point-wise or spatial (one-, two-, three-, or multi-dimensional). It can be algebraic, harmonic, or a finite-difference equation. A model with one argument is called single-dimensional and multi-dimensional when it has more than one argument. If the model is constructed from the observed data in which the location of the sensors is not known, then it is point-wise. If the data contain the information concerning the sensor locations, then the model is spatial or distributive parametric. Spatial models require the presence of at least three spatial locations on each axis.

In the theory of mathematical physics, physical field is represented with differential or integro-differential equations; linear differential equations have nonlinear solutions. For solving such equations numerically, discrete analogues in the form of finite difference equations are built up. This is done by considering two subsequent cubicles for analogue of first derivative, three cubicals for analogue of second derivative, and so on. As the higher analogues are taken into consideration, the number of arguments in the model structure are

correspondingly increased. In other words, the physical field is discretized in terms of the discrete analogues or patterns. To widen the sorting, it is worthwhile to adopt different patterns (consisting of arguments) starting from simple two-cubical patterns to patterns with the possibility of all polynomials. Higher-ordered arguments and paired sorting of patterns and nonlinear polynomials give the possibility of fully reexamining the majority of partial polynomials for representing the physical field. By sorting, it is easier to "guess" the linear character of a finite-difference equation rather than the nonlinearity of its solution. This reduces the sorting of basis functions. The collection of data with regard to the pattern structures, presentation to the algorithm, and evaluation of the patterns are considered as important aspects of the inductive modeling.

1 FINITE-DIFFERENCE PATTERN SCHEMES

Discrete mathematics is based on replacing differentials by finite differences measured at the mesh points of a rectangular spatial mesh or grid. For example, the axes of the three dimensional coordinates x, y, z are discretized into equal sections (steps), usually taken as the unit measurement of $Ax = 1$, $\Delta y = 1$, and $\Delta z = 1$. The building up of finite difference equations are based on the construction of patterns or elementary finite difference schemes.

A geometric pattern that indicates the points of the field used to form the equation structure is called elementary pattern. A pattern is a finite difference scheme that connects the value of a given function at the kth point with the value of several other arguments at the neighboring points of the spatial mesh. The pattern for the solution of a specific problem can be determined in two ways: (i) by knowing the physics of the plant (the deductive approach), (ii) by sorting different possible patterns to select the best suited one by an external criterion (the inductive approach). The former is out of the scope of this book and emphasis is given to the latter through the use of inductive learning algorithms.

In a system where y is an output variable and x is an independent variable, a pattern with mesh points within a step apart is shown in Figure 4.1. The general form of the equation representing the complete pattern is

$$y_{i,j,k} = f(y_{i+1,j,k}, y_{i-1,j,k}, y_{i,j+1,k}, y_{i,j-1,k}, y_{i,j,k+1}, y_{i,j,k-1},$$
$$x_{i+1,j,k}, x_{i-1,j,k}, x_{i,j+1,k}, x_{i,j-1,k}, x_{i,j,k+1}, x_{i,j,k-1}). \tag{4.1}$$

This will be more complicated if the delayed arguments are considered by introducing the time axis t as a fourth dimension.

$$y_{i,j,k}^t = f(y_{i+1,j,k}^t, y_{i-1,j,k}^t, y_{i,j+1,k}^t, y_{i,j-1,k}^t, y_{i,j,k+1}^t, y_{i,j,k-1}^t, y_{i,j,k}^{t-1}$$
$$x_{i+1,j,k}^t, x_{i-1,j,k}^t, x_{i,j+1,k}^t, x_{i,j-1,k}^t, x_{i,j,k+1}^t, x_{i,j,k-1}^t, x_{i,j,k}^{t-1}). \tag{4.2}$$

In actual physical problems, most of these arguments are absent because they do not influence the dependent variable. This is the difference between the actual pattern and the complete pattern.

For example, in the linear problem of two-dimensional $(x$ and $t)$ turbulant diffusion we have

$$\frac{\partial q}{\partial t} + u\frac{\partial q}{\partial x} - K\frac{\partial^2 q}{\partial x^2} = 0, \tag{4.3}$$

where u is the flow velocity and K is the diffusion coefficient. The discrete analogue of this equation can be written as

$$(q_i^{t+1} - q_i^t) + \gamma_1(q_{i+1}^t - q_{i-1}^t) - \gamma_2(q_{i+1}^t - 2q_i^t + q_{i-1}^t) = 0, \tag{4.4}$$
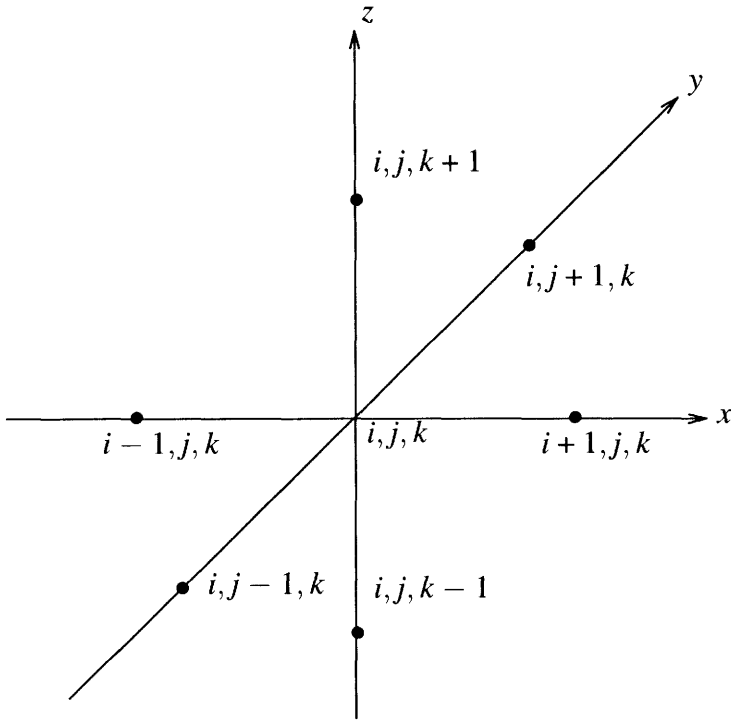
Figure 4.1. "Complete" pattern in (x, y, z) coordinates

where $\gamma_1 = \frac{\tau u}{2h}$, and $72 = \frac{\tau K}{h^2}$. In other words, we use a pattern with three arguments in the functional form of

$$q_i^{t+1} = f(q_i^t, q_{i+1}^t, q_{i-1}^t). \tag{4.5}$$

If we consider the Fokker-Planck equation, which takes the above diffusion equation with variable diffusion coefficient K as

$$\frac{\partial q}{\partial t} + u \frac{\partial q}{\partial x} - \frac{\partial^2 K q}{\partial x^2} = 0, \tag{4.6}$$

then the discrete counterpart is taken as

$$(q_i^{t+1} - q_i^t) + \gamma_1(q_{i+1}^t - q_{i-1}^t) - \gamma_2(K_i^{t+1} q_{i+1}^t - 2K_i^t q_i^t + K_{i-1}^t q_{i-1}^t) = 0, \tag{4.7}$$

where $\gamma_1 = \frac{\tau u}{2h}$, and $\gamma_2 = \frac{\tau}{h^2}$. The pattern consists of the functional form of

$$q_i^{t+1} = f(q_i^t, q_{i+1}^t, q_{i-1}^t, K_i^t, K_{i+1}^t, K_{i-1}^t). \tag{4.8}$$

Usually the dynamic equation is expressed in the form of a sum of two parts: the left side "operator" and the right side "source function" or "remainder." In the problem of turbulant diffusion we can write the equation as

$$\frac{\partial q}{\partial t} + u \frac{\partial q}{\partial x} - K \frac{\partial^2 q}{\partial x^2} = f(x, t), \tag{4.9}$$

where the left side is the "operator" and $f(x, t)$ is the "remainder." The discrete analogue of this equation takes the form of

$$q_i^{t+1} = f(q_i^t, q_{i+1}^t, q_{i-1}^t) + f(x, t), \tag{4.10}$$

where x and t are the coordinate values of q_i^{t+1} on the grid. $f(x, t)$ can be considered as a linear trend in x and t; for example, $f(x, t) = a_0 + a_1 x + a_2 t$.

For solving very complex problems using the inductive approach, complete polynomials with a considerable number of terms should be used. Usually if the reference function or "complete" polynomial has less than 20 arguments, the combinatorial algorithm is used to select the best model. If it has more than or equal to 20 arguments, the multilayer algorithm is used, depending on the capacity of the computer.

1.1 Ecosystem modeling

The following examples illustrate the identification of one-dimensional and multi-dimensional physical fields related to the processes in the ecosystem.

Example 1.   Usually model optimization refers to the choice of the number of time delays considering a one-dimensional problem in time t. For the synthesis of the optimal model, the number of time delays must be gradually increased until the selection criterion decreases. The optimal model corresponds to the global minimum of the external criterion.

Let us consider identification of concentration of dissolved oxygen (DO) and biochemical oxygen demand (BOD). The discrete form of the Streeter-Phelps law [9] is taken along with the experimental data as

$$q^{t+1} = k_1 q_{max} + (1 - k_1)q^t - k_2 u^t$$
$$u^{t+1} = u^t - k_2 u^t, \tag{4.11}$$

where q^t is the DO concentration in mg/liter at time t; q_{max} is the maximum DO concentraion; u^t is the BOD in mg/liter at time t; $k\textbackslash$ is the rate of reaeration per day; and k_2 is the rate of BOD decrease per day.

Complete polynomials are considered as

$$q^{t+1} = f(q^t, q^{t-1}, q^{t-2}, \cdots, q^{t-\tau_1}, u^t, u^{t-1}, u^{t-2}, \cdots, u^{t-\tau_2})$$
$$u^{t+1} = f(q^t, q^{t-1}, q^{t-2}, \cdots, q^{t-\tau_1}, u^t, u^{t-1}, u^{t-2}, \cdots, u^{t-\tau_2}), \tag{4.12}$$

where τ_1 and T2 are time delays taken as three.   The combinatorial algorithm is used to generate all possible combinations of partial models.   The data is collected in daily intervals—65 data points are used in training and 15 points are kept for examining the predictions. The combined criteria of "minimum bias (η_{bs}) plus prediction (i)" is used for selecting the best model in optimal complexity. The optimal models obtained are

$$q^{t+1} = 1.3350 + 0.8142 q^t - 0.00001 u^t$$
$$u^{t+1} = u^t - 0.2545 u^t + 0.1471 q^{t-3}. \tag{4.13}$$

The prediction errors for the model of DO concentrations is 7% and for the model of BOD, 14%. This shows how a physical law can be discovered using the inductive learning approach.

The interpolation region is the space inside the three-dimensional grid with points located at the measuring stations and which lay inside the time interval of the experimental data. The extrapolation region in general lies outside the grid, and the prediction region lies in the future time outside the interpolation region. Usually, the interpolation region is involved in the training of the object. According to the Weiesstrass theorem, the characteristic feature of the region is that any sufficiently complicated curve fits the experimental data with any

desired accuracy. In the extrapolation and prediction regions, the curves quickly diverge, forming so-called "fan" of predictions. The function with optimal complexity must have the best agreement with the future process development.

The following example illustrates modeling of a two-dimensional (x, t) physical field of an ecosystem for identification, prediction, and extrapolation. This shows that the optimal pattern and optimal remainder can be found by sifting all possible patterns, with the possible terms of "source function" using the multilayered inductive approach and the sequential application of minimum bias and prediction criteria.

Example 2.   The variables (i) dissolved oxygen q', (ii) biochemical oxygen demand u', and (iii) temperature T' are measured at three stations of a water reservoir at a depth of 0.5 m. The measurements are taken eight times at 4-week intervals. As a first step, with the measured data, a uniform two-dimensional grid (16 x 16) of data is prepared by using quadratic interpolation and algebraic models [46].

Here two types of problems are considered: prediction and extrapolation problems. The model formulations are considered as combination of source and operator functions with the following arguments.

(i) Prediction problem:

$$q_i^{t+1} = f_1(x, t) + f_2(q_i^t, q_i^{t-1}, q_i^{t-2}, q_{i-1}^t, q_{i+1}^t, u_i^t, u_i^{t-1}, u_i^{t-2}, u_{i-1}^t, u_{i+1}^t, T_i^t)$$
$$u_i^{t+1} = f_3(x, t) + f_4(q_i^t, q_i^{t-1}, q_i^{t-2}, q_{i-1}^t, q_{i+1}^t, u_i^t, u_i^{t-1}, u_i^{t-2}, u_{i-1}^t, u_{i+1}^t, T_i^t). \qquad (4.14)$$

(ii) Extrapolation problem:

$$q_{i+1}^t = f_5(x, t) + f_6(q_i^t, q_{i-1}^t, q_{i-2}^t, q_i^{t-1}, q_i^{t+1}, u_i^t, u_{i-1}^t, u_{i-2}^t, u_i^{t-1}, u_i^{t+1}, T_i^t)$$
$$u_{i+1}^t = f_7(x, t) + f_8(q_i^t, q_{i-1}^t, q_{i-2}^t, q_i^{t-1}, q_i^{t+1}, u_i^t, u_{i-1}^t, u_{i-2}^t, u_i^{t-1}, u_i^{t+1}, T_i^t). \qquad (4.15)$$

The data tables are prepared in the order of the output and input variables in the function. Each position of the pattern gives one data measurement of the initial table.

The complete polynomial in each case is considered second-degree polynomial. For example, the complete polynomial for prediction of DO concentration is

$$q_i^{t+1} = (a_0 + a_1 x + a_2 t)$$
$$+ (a_3 q_i^t + a_4 q_i^{t-1} + \cdots + a_7 q_{i+1}^t + a_8 u_i^t + a_9 u_i^{t-1} + \cdots + a_{12} u_{i+1}^t + a_{13} T_i^t$$
$$+ a_{14} q_i^{t^2} + \cdots + a_{24} T_i^{t^2} + a_{25} q_i^t q_i^{t-1} + \cdots + a_{79} u_{i+1}^t T_i^t). \qquad (4.16)$$

This has 80 terms: 14 linear terms, 11 square terms, and 55 covariant terms. A multilayer algorithm is used. In the first layer, C_{80}^2 (=3160) partial models are formed and the best 80 of them are selected using the minimum bias criterion. It is repeated layer by layer until the criterion decreases. At the last layer 20 best unbiased models are selected for considering long-term predictions. Finally, the optimal models for each problem are chosen with regard to the combined criterion "minimum bias (η_{bs}) plus prediction ($c3$)."

For prediction:

$$q_i^{t+1} = 12.4306 - 4.6477 u_i^t + 0.1615 q_i^{t-2} u_i^t + 0.8896 u_i^{t^2} - 0.0035 u_i^t u_i^{t+1} + 0.0004 t;$$
$$c3 = 0.00012$$
$$u_i^{t+1} = 1.1149 + 0.0200 u_i^{t-1} T_i^t + 0.0042 u_{i+1}^t T_i^t;$$
$$c3 = 0.0003. \qquad (4.17)$$

For extrapolation:

$$q_{i+1}^t = 9.5237 + 0.0937u_i^t u_{i-2}^t + 0.0031u_i^t T_i^t$$
$$+0.2500u_{i-1}^t u_{i-2}^t - 0.1403u_{i-1}^t u_i^{t+1} - 0.0271u_{i-2}^{t^2}$$
$$+0.0392u_{i-2}^t q_i^{t-1} - 0.1782u_{i-2}^t u_i^{t-1} - 0.0288u_i^{t-1^2}$$
$$-0.1046u_i^{t-1} u_i^{t+1};$$
$$c3 = 0.00015$$
$$u_{i+1}^t = -0.1798 + 1.1573u_i^t - 0.1124u_i^{t^2} + 0.000966u_i^{t-1} T_i^t;$$
$$c3 = 0.000075. \tag{4.18}$$

The accuracy of these models is considerably higher for long-term predictions or extrapolations of up to 10 to 20 steps ahead (the error is not over 20%).

In the literature, "Cassandra predictions" (prediction of predictions) are suggested under specific variations in the data [1], [30]. As we all know, the fall of Troy came true as predicted by Cassandra, the daughter of King Priam of Troy, while the city was winning over the Hellenes. It is important that the chosen model must predict a drop/rise in the very near future on the basis of monotonically increasing/ decreasing data, correspondingly. If the model represents the actual governing law of the system, it will find the inflection point and predict it exactly. Usually, the law connecting the variables is trained in the interpolation region to represent the predicting variable. This does not remain constant in the extrapolation region. "Cassandra predictions" explains that it is possible to identify a governing law within the reasonable noise levels on the basis of past data using inductive learning algorithms. For example, let us consider the model formulation as

$$q = f(u, t)$$
$$u_j = f_j(u), \quad j = 1, 2, \cdots, m, \tag{4.19}$$

where q is the output variable, u is the vector of input variables, and t is the current time. The secret of obtaining the "Cassandra predictions" is to build up the function that has the characteristics of variable coefficients.

To identify a gradual drop/rise in the data at a later time by predicting q, one has to obtain the predicted values of u_j using the second function and use these predicted values in predicting q. In other words, it works as prediction of predictions. However, the "Cassandra predictions" demand more unbiased models ($0 < \eta_{bs} < 0.05$). For an unbiased equation $q = f(u, t)$ to have an extremum at an prediction point (u^{tn}, t_n), where t_n is the time the prediction is made, it is expected that either a decrease or increase occurs in the value of q. If the data is too noisy, it restricts the interval length of the prediction time.

Here another example is given to show that the choice of a pattern and a remainder uniquely determines the "operator" and the "source function" of a multidimensional object.

Example 3. Identification of the mineralization field of an artesian aquifer in the steppe regions of the Northern Crimea is considered [56], [57].

We give a brief description of the system; a schematic diagram of the object with observation net of wells is shown in Figure 4.2. The coordinate origin is located at an injection well. The problem of liquid filtration from a well operating with a constant flow rate is briefed as below: an infinite horizontal seam of constant power is explored by a vertical well of negligibly small radius. Initially the liquid in the seam is constant and the liquid begins to flow upwards at a constant volumetric rate. From a hydrological point of view, the object of investigation is a seam of water-soaked Neocene lime of 170 m capacity,
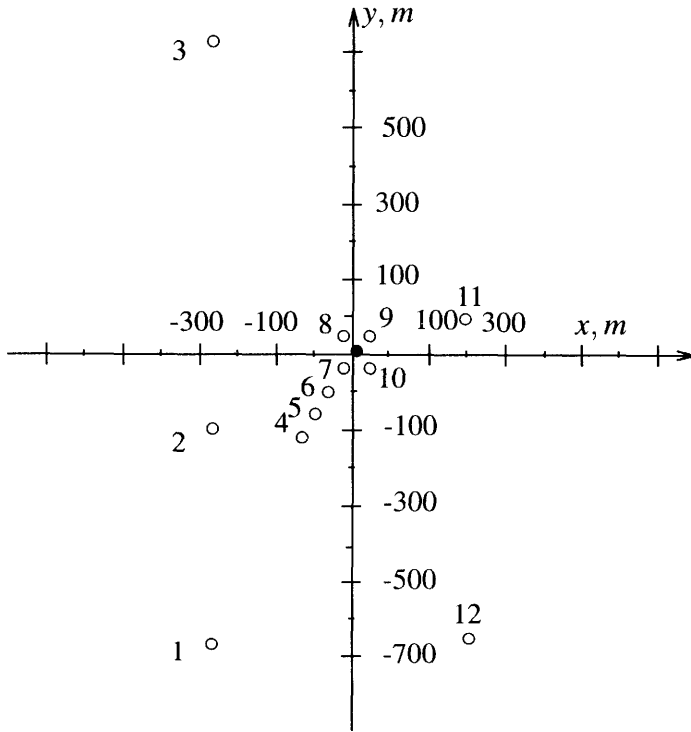
Figure 4.2.   Location of observation wells

bounded from above and below by layers of clay that are assumed to be impermeable to water—in the sense that it does not permitting significant passage of liquid. The average depth of the seam is 60 m. The piezometric levels used for exploring the seam are fixed at a depth ranging from 0 to 7 m below the earth's surface. Their absolute markings relative to sea level vary between 0.8 and 4.0 m. In the experimental region, the water flow has a minor deviation in the northernly direction—this agreeing with the regional declination of the seam in the direction of the flow of subterranean waters of this area. According to the prevailing hypothesis, the Black sea is regarded as a run-off region—this is confirmed by the intrusion of salty waters into the aquifer, accompanied by a lowering of the water head in the boundary region as a result of high water extraction for consumption. The aquifer has an inhomogeneous structure, that consists of porous lime with cracks whose permeability varies along the vertical from 8 to 200 m per 24-hour period. The mineralization of the water varies along the vertical from 2 to 3 g/l (as the surface of the seam) to 6 g/l at a depth of 100 m from the surface.

The physical law that is considered as a dynamic model representing the mineralization is the conservation of mass. In hydrodynamics this principle is called continuity law or "principle of close action." The equation is expressed as

$$\frac{\partial q}{\partial t} + u\frac{\partial q}{\partial x} + v\frac{\partial q}{\partial y} + w\frac{\partial q}{\partial z} - [\frac{\partial}{\partial x}(K_x\frac{\partial q}{\partial x}) + \frac{\partial}{\partial y}(K_y\frac{\partial q}{\partial y}) + \frac{\partial}{\partial z}(K_z\frac{\partial q}{\partial z})]$$

$$= Q_q(x, y, z, t) + P(x, y, z), \tag{4.20}$$

where u, v, and w are the velocity components, $K_x, K_y,$ and K_z are the diffusion coefficients,

Q_q is a source function for the ith element, and P is a function representing the interaction of the terms (it is called "remainder").

This can be expressed in the discrete analogue as follows:

$$(q_{i,j,k}^{t+1} - q_{i,j,k}^t) + \gamma_1[u(q_{i+1,j,k}^t - q_{i,j,k}^t) + v(q_{i,j+1,k}^t - q_{i,j,k}^t) + w(q_{i,j,k+1}^t - q_{i,j,k}^t)]$$

$$-\gamma_2[K_x(q_{i+1,j,k}^t - 2q_{i,j,k}^t + q_{i-1,j,k}^t) + K_y(q_{i,j+1,k}^t - 2q_{i,j,k}^t + q_{i,j-1,k}^t)+$$

$$K_z(q_{i,j,k+1}^t - 2q_{i,j,k}^t + q_{i,j,k-1}^t)] \ = f(x,y,z,t), \tag{4.21}$$

where: $\gamma_1 = \tau/h$, $\gamma_2 = \tau/h^2$; $f(x,y,z,t)$ is taken in the general form as

$$f(x,y,z,t) = P(x,y,z) + Q_q(x,y,z,t)$$

$$= a_0 + a_1 x + a_2 y + a_3 z + a_4 q_{i,j-1,k}^{t-1} + a_5 q_{i,j,k}^t + a_6 \frac{Qe^{-\frac{0.35R_i}{t}}}{\sqrt{t4\pi R_i}} \tag{4.22}$$

in which Q is the water flow rate in cubic meters during time Δt, R is the distance of a point with coordinates x, y, z from the injection well, $R = \sqrt{(x^2 + y^2 + z^2)}$, $z = z - z_0$, t is the running time from the beginning of the operation (in 24-hour periods), and 0.35 is the optimal value determined for porosity of the medium.

There exists a unique correspondence between the adopted pattern and dynamic equation of the physical field. The choice of pattern determines the structure of the dynamic equation, but only of its left side operator and not of the right-side part of the equation. The optimal pattern is determined by the inductive approach using an external criteria. The pattern must yield the deepest minimum of the criteria. In other words, the optimization problem is reduced to a selection of a pattern. The inductive approach is of interest because it leads to discovery of new properties of the system. Simulation of complex systems by this approach is very convenient for examining a large number of percolation hypotheses and selecting the best one. The selection of the arguments in the algorithm is directly related to the percolation hypothesis to be adopted and must have a sufficiently wide scope. In this example, the optimal selection of arguments is based on sorting of a large number of patterns.

The above finite difference equation is considered a reference function representing the "complete" pattern. All the partial models corresponding to the partial patterns can be obtained by zeroing in the terms of the reference function as is done in the "structure of functions." This means that a specified pattern determines the operator of the left side equation, and not the remainder. For example, for pattern no. 1 the partial function is given as

$$(q_{i,j,k}^{t+1} - q_{i,j,k}^t) + \frac{\tau w}{h}(q_{i,j,k+1}^t - q_{i,j,k}^t) + \frac{\tau u}{h}(q_{i+1,j,k}^t - q_{i,j,k}^t)-$$

$$K_x(q_{i+1,j,k}^t - 2q_{i,j,k}^t + q_{i-1,j,k}^t) \ = f(x,y,z,t). \tag{4.23}$$

Overall, there are 13 coefficients for the complete pattern. $2^{13} - 1$ partial models are generated if the combinatorial algorithm is used. It is equivalent to the optimal selection of arguments based on sorting a sufficiently large number of patterns. The difference data is measured from the given region with interpolation of the q value at the intermediate points of the mesh. The problem is reduced to the selection of an optimal pattern among a set of

Table 4.1.   Values of the minimum bias criterion

No.	Value	No.	Value	No.	Value
1	0. 08239	8	0. 04669	15	0. 04669
2	0. 08239	9	0. 04669	16	0. 04669
3	0. 08239	10	0. 06546	17	0. 04669
4	0. 11075	11	0. 06545	18	0. 04669
5	0. 04669	12	0. 06545	19	0. 04669
6	0. 04669	13	0. 04669	20	0. 04669
7	0. 09652	14	0. 04669	21	0. 09674

patterns; i.e., a unique model that yields the deepest minimum of the combined criterion is selected.

$$c1^2 = \bar{\eta}_{bs}^2 + \bar{\Delta}^2(W/A), \tag{4.24}$$

where η_{bs} is the normalized minimum bias criterion and $\bar{\Delta}(W/A)$ is the normalized regularity criterion.

The total number of feasible patterns is $2^6 - 1 = 63$. Some of the patterns are shown in the Figure 4.3. Table 4.1 exhibits the values of the minimum bias criterion for these patterns. The optimal pattern with regard to the combined criterion $c\backslash$ is found to be pattern 9. The optimal equation is

$$q_{i,j,k}^{t+1} = 1.325 q_{i,j,k}^{t} + 14.13 \frac{q_{i,j+1,k}^{t} - 2q_{i,j,k}^{t} + q_{i,j-1,k}^{t}}{h^2} - 2.15 \frac{q_{i,j+1,k}^{t} - q_{i,j-1,k}^{t}}{2h}$$

$$- 0.08747 q_{i,j-1,k}^{t-1} - 0.002716 \frac{Qe^{-\frac{0.35 R_i}{t}}}{\sqrt{t 4 \pi R_i}}. \tag{4.25}$$

The last two terms in the equation correspond to the remainder function.

Stability analysis

The stability analysis of equations of the form above was carried out. It was proved that stability with regard to the initial data can be realized under the conditions

$$(i) \ \frac{\tau K_y}{h^2} < \frac{1}{2},$$

$$(ii) \ v^2 < \frac{2K_y}{\tau}\left(1 - \frac{2\tau K_y}{h^2}\right), \tag{4.26}$$

where the former is the well-known stability condition and the latter is the condition for interconnection of the coefficients of the finite-difference equation.

2   COMPARATIVE STUDIES

As a continuation of our study on elementary pattern structures, some examples of correspondence between linear differential equations and their finite-difference analogues are given in Tables 4.2 and 4.3. Here time t is shown as one of the axes (see Figure 4.4).

For physical fields some deterministic models are usually known, they are given by differential or integro-differential equations. Such equations from the deterministic theories

No.	Pattern	No.	Pattern	No.	Pattern
1	$k+1$; $i+1$ — i,j,k — $i-1$	8	$j+1$; $i+1$ — i,j,k ; $j-1$ $k-1$	15	$k+1$ $j+1$; $i+1$ — i,j,k — $i-1$; $k-1$
2	$i+1$ i,j,k $i-1$; $k-1$	9	$k+1$ $j+1$; $i+1$ — i,j,k ; $j-1$ $k-1$	16	$k+1$ $j+1$; i,j,k — $i-1$; $j-1$
3	$k+1$; $i+1$ — i,j,k — $i-1$; $k-1$	10	$k+1$; $i+1$ — i,j,k — $i-1$; $j-1$	17	$j+1$; i,j,k — $i-1$; $j-1$ $k-1$
4	$k+1$ $j+1$; i,j,k ; $j-1$	11	$i+1$ i,j,k $i-1$; $j-1$ $k-1$	18	$k+1$ $j+1$; i,j,k — $i-1$; $j-1$ $k-1$
5	$j+1$; i,j,k ; $j-1$ $k-1$	12	$k+1$; $i+1$ — i,j,k — $i-1$; $j-1$ $k-1$	19	$k+1$ $j+1$; $i+1$ — i,j,k — $i-1$; $j-1$
6	$k+1$ $j+1$; i,j,k ; $j-1$ $k-1$	13	$k+1$ $j+1$; $i+1$ — i,j,k — $i-1$	20	$j+1$; $i+1$ — i,j,k — $i-1$; $j-1$ $k-1$
7	$k+1$ $j+1$; $i+1$ — i,j,k ; $j-1$	14	$j+1$; $i+1$ — i,j,k — $i-1$; $k-1$	21	$k+1$ $j+1$; $i+1$ — i,j,k — $i-1$; $j-1$ $k-1$

Figure 4.3.   Certain patterns among 63 feasible patterns

Figure 4.4.   Field in coordinates of x and t

may be used for choosing the arguments and functions for a "complete" reference function. A complete pattern is made from the deterministic equation pattern by increasing its size by one or two cells along all axes; i.e., the equation order is increased by one or two to let the algorithm choose a more general law.

2.1   Double sorting

There are two ways of enlarging the sorting of arguments. One way is as shown in Tables 4.2 and 4.3 and starts from the simplest to the more complex pattern. Another way is by considering higher-order arguments for each pattern and sorting them. The polynomials with higher-order terms provide a more complete view of the set of possible polynomials. The complexity of the polynomials increases as the delayed and other input variables are added to them. For example, shown are the pointwise models of a variable q using simple patterns. Without delayed arguments, it is

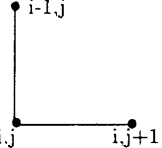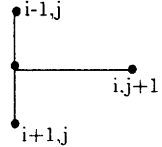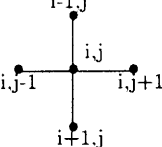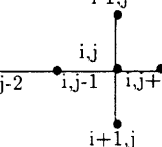$$q^{t+1} = f(q^t) = a_0 + a_1 q^t + a_2 q^{t^2} ; \tag{4.27}$$

with one delayed argument it is

$$q^{t+1} = f(q^t, q^{t-1}) = a_0 + a_1 q^t + a_2 q^{t-1} + a_3 q^{t^2} + a_4 q^{t-1^2} + a_5 q^t q^{t-1}, \tag{4.28}$$

and with two delayed arguments,

$$\begin{aligned} q^{t+1} &= f(q^t, q^{t-1}, q^{t-2}) \\ &= a_0 + a_1 q^t + a_2 q^{t-1} + a_3 q^{t-2} + a_4 q^{t^2} + a_5 q^{t-1^2} + a_6 q^{t-2^2} \\ &\quad + a_7 q^t q^{t-1} + a_8 q^t q^{t-2} + a_9 q^{t-1} q^{t-2}. \end{aligned} \tag{4.29}$$

Table 4.2.   Sorting of elementary patterns and data Tables

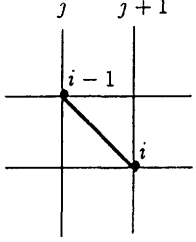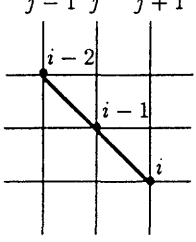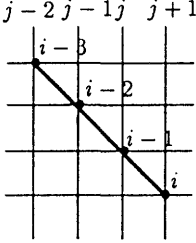| Pattern	Model and its Discrete Analogue	Data Table Representation
i,j •——— i,j+1	$\frac{\partial q}{\partial t} + a_1 q = f(x,t)$, $q_i^{t+1} = f_1(x,t) + f_2(q_i^t)$	$\boxed{q_i^{t+1}}\ \boxed{q_i^t}$
i-1,j • | i,j •——— i,j+1	$\frac{\partial q}{\partial t} + a_1 \frac{\partial q}{\partial x} + a_2 q = f(x,t)$, $q_i^{t+1} = f_1(x,t) + f_2(q_i^t, q_{i-1}^t)$	$\boxed{q_i^{t+1}}\ \boxed{q_i^t}\ \boxed{q_{i+1}^t}$
i-1,j • i,j •——— i,j+1 i+1,j •	$\frac{\partial^2 q}{\partial t^2} + a_1 \frac{\partial^2 q}{\partial x^2} + a_2 \frac{\partial q}{\partial x} + a_3 q = f(x,t)$, $q_i^{t+1} = f_1(x,t) + f_2(q_i^t, q_{i+1}^t, q_{i-1}^t)$	$\boxed{q_i^{t+1}}\ \boxed{q_i^t}\ \boxed{q_{i+1}^t}\boxed{q_{i-1}^t}$
i-1,j i,j i,j-1 •——+——• i,j+1 i+1,j	$\frac{\partial^2 q}{\partial t^2} + a_1 \frac{\partial q}{\partial t} + a_2 \frac{\partial^2 q}{\partial x^2} + a_3 \frac{\partial q}{\partial x}$ $+ a_4 q = f(x,t)$, $q_i^{t+1} = f_1(x,t) + f_2(q_i^t, q_{i+1}^t, q_{i-1}^t, q_i^{t-1})$	$\boxed{q_i^{t+1}}\ \boxed{q_i^t}\ \boxed{q_{i+1}^t}\boxed{q_{i-1}^t}\boxed{q_i^{t-1}}$
i-1,j i,j i,j-2 i,j-1 i,j+1 i+1,j	$\frac{\partial^3 q}{\partial t^3} + a_1 \frac{\partial^2 q}{\partial t^2} + a_2 \frac{\partial q}{\partial t} + a_3 \frac{\partial^2 q}{\partial x^2} + a_4 \frac{\partial q}{\partial x}$ $+ a_5 q = f(x,t)$, $q_i^{t+1} = f_1(x,t)$ $+ f_2(q_i^t, q_{i+1}^t, q_{i-1}^t, q_i^{t-1}, q_i^{t-2})$	$\boxed{q_i^{t+1}}\ \boxed{q_i^t}\ \boxed{q_{i+1}^t}\boxed{q_{i-1}^t}\boxed{q_i^{t-1}}\boxed{q_i^{t-2}}$

Similarly, in case of two variables q and x, the formulations

$$q^{t+1} = f(q^t, x^t),$$
$$q^{t+1} = f(q^t, x^t, q^{t-1}, x^{t-1}),$$
$$q^{t+1} = f(q^t, x^t, q^{t-1}, x^{t-1}, q^{t-2}, x^{t-2}), \qquad (4.30)$$

and so on, gradually increase their complexity. In the same way, spatial models can be developed by considering the delayed and higher-order terms. Sorting of all partial polynomials means generation of all combinations of input arguments for "structure of functions" using the combinatorial algorithm. One can see that the sorting is done in two aspects: one is pattern-wise sorting and the other is orderwise sorting. This is called "double sorting." These are used below for modeling of simulated air pollution fields in the example given.

One should distinguish between Tables of measuring stations and interpolated initial data. Different patterns result in different settings of numerical field of the Table. The measurement points are ordered as shown in the "data representation" (Tables 4.2 and 4.3). Each position of a pattern on the field corresponds to one measurement point in the data table. Each pattern results in its own data table; there are as many tables as there are patterns compared. Tables resulting from the displacement of patterns with respect to the numerical

Table 4.3. Sorting of "diagonal" type patterns and data tables

'Diagonal' Type Pattern	Model and its Discrete Analogue	Data Table Representation
j $j+1$, $i-1$, i (diagonal pattern)	$\frac{\partial q}{\partial t} + a_1 \frac{\partial q}{\partial x} + a_2 q = f(x,t),$ $q_i^{t+1} = f_1(x,t) + f_2(q_{i-1}^t)$	q_i^{t+1} q_{i-1}^t
$j-1$ j $j+1$, $i-2$, $i-1$, i (diagonal pattern)	$\frac{\partial^2 q}{\partial t^2} + a_1 \frac{\partial^2 q}{\partial x^2} + a_2 \frac{\partial q}{\partial t} + a_3 \frac{\partial q}{\partial x}$ $+ a_4 q = f(x,t),$ $q_i^{t+1} = f_1(x,t) + f_2(q_{i-1}^t, q_{i-2}^{t-1})$	q_i^{t+1} q_{i-1}^t q_{i-2}^{t-1}
$j-2$ $j-1$ j $j+1$, $i-3$, $i-2$, $i-1$, i (diagonal pattern)	$\frac{\partial^3 q}{\partial t^3} + a_1 \frac{\partial^3 q}{\partial x^3} + a_2 \frac{\partial^2 q}{\partial t^2} + a_3 \frac{\partial^2 q}{\partial x^2} + a_4 \frac{\partial q}{\partial t}$ $+ a_5 \frac{\partial q}{\partial x} + a_6 q = f(x,t),$ $q_i^{t+1} = f_1(x,t) + f_2(q_{i-1}^t, q_{i-2}^{t-1}, q_{i-3}^{t-2})$	q_i^{t+1} q_{i-1}^t q_{i-2}^{t-1} q_{i-3}^{t-2}

field of data are divided for external criteria. The best pattern provides the deepest minimum of the criteria.

2.2 Example—pollution studies

Example 4. Modeling of air pollution field. Three types of problems are formulated [47] for modeling of the pollution field using: (i) the data of a single station, (ii) the data about other pollution components, and (iii) combining both.

In the first problem, the finite-difference form of the model is found by using experimental data through sorting the patterns and using the higher-ordered arguments. The number of terms of the "complete" equation is usually much greater than the total number of data points. In the second problem, the arguments in the finite difference equations are chosen as they correspond to the "input-output matrix" [122] of pollution components; whereas in the third problem, it corresponds to the "input-output matrix" of pollution components and sources. Three problems can be distinguished based on the choice of arguments. The first problem is based on the "principle of continuity or close action;" the second, which

is opposite to the first, is based on the "principle of remote action." The third is based on both principles "close and remote actions."

The number of stations that register pollution data increases each year, but sufficient data are still not available. The inductive approach requires a relatively small number of data points and facilitates significant noise stability according to the choice of an external criterion. The mathematical formulations of a physical field described in connection with the above problems compare the different approaches. Additional measurements are used for refinement of each specific problem. In representing the pollution field, station data, data about location, intensity and time of pollutions are used. The choice of output quantity and input variables determines the formulations. This depends on the problem objective (interpolation, extrapolation, or prediction) and on availability of the experimental data.

Before explaining the problem formulations, a brief description about the formation of "input-output matrix" is given here.

Input-output matrix

The "input-output matrix" is estimated based on the linear relationships between the pollution sources u and pollution concentrations q using the observation data at the stations. The matrix is used as a rough model of the first approximation and the differences between the actual outputs q and estimated outputs using the inductive algorithm. The pollution model in vector form is given as $q = f.u$, where q is the pollution concentration at a station, u is the intensity of the pollution source, and f is a coefficient that accounts for various factors relating to the source and diffusion fields—f is regarded as a function of the relative coordinates between pollution source and the observation station. Other factors, such as terrain and atmospheric count, are implicitly taken into consideration in determining f on the basis of observation data.

For a set of sources $u_j, j = 1, 2, \cdots, m$, the pollution concentration for each observation station $q_i, i = 1, 2, \cdots, n$ is represented by

$$q_i = \sum_{j=1}^{m} f_i(x_{ij}, y_{ij}) u_j; \quad i = 1, 2, \cdots, n, \tag{4.31}$$

where

$$x_{ij} = x_i^r - x_j^s; \quad i = 1, 2, \cdots, n; \ j = 1, 2, \cdots, m$$
$$y_{ij} = y_i^r - y_j^s; \quad i = 1, 2, \cdots, n; \ j = 1, 2, \cdots, m.$$

q_i is the pollution concentration at the ith station; u_j is the intensity of the jth source; x_i^r, y_i^r are the coordinates of the ith station; x_j^s, y_j^s are the coordinates of the jth source; n is the number of stations and m is the number of sources.

This can be written in matrix form as

$$q = F.u, \tag{4.32}$$

where

$$q^T = (q_1, q_2, \cdots, q_n), \quad u^T = (u_1, u_2, \cdots, u_m) \text{ and}$$

$$F = \begin{pmatrix} f_{11} & f_{12} & \cdots & f_{1m} \\ f_{21} & f_{22} & \cdots & f_{2m} \\ & \cdots & & \\ f_{n1} & f_{n2} & \cdots & f_{nm} \end{pmatrix}.$$

Here F is called the "input-output matrix." Each element f_{ij} can be described by

$$f_{ij} = a_{0j} + a_{1j}x_{ij} + a_{2j}y_{ij} + a_{3j}x_{ij}^2 + a_{4j}y_{ij}^2 + a_{5j}x_{ij}y_{ij} + a_{6j}e^{-\alpha_j\sqrt{x_{ij}^2+y_{ij}^2}}, \tag{4.33}$$

which is estimated by using spatially distributed data. The equation obtained for one source can be used for all other pollution sources. The matrix F is determined by applying f_{ij} to each source. This is treated as a "rough" model because of its dependence on the coordinate distances in the field. This is used to estimate the linear trend part of the system, the remainder part, which is the unknown nonlinear part of the system, is described by

$$\Delta q_i = \frac{1}{m}\sum_{j=1}^{m} g_j(x_{ij}, y_{ij}); \quad i = 1, 2, \cdots, N, \tag{4.34}$$

where

$$x_{ij} = x_i^r - x_j^s; \quad i = 1, 2, \cdots, N; \; j = 1, 2, \cdots, m$$
$$y_{ij} = y_i^r - y_j^s; \quad i = 1, 2, \cdots, N; \; j = 1, 2, \cdots, m.$$

$\Delta q_i (= q_i - \hat{q}_i)$ is the remainder at the ith point; N is the total number of points on the (x, y) grid; the function $g_j(x_{ij}, y_{ij})$ is described by a polynomial of a certain degree in x_{ij} and y_{ij}. The remainder equation is estimated as an average of m source models that is identified by using an inductive algorithm. The predictions obtained from the linear trend or rough model are corrected with the help of a remainder model.

Problem formulations

The first problem is formulated to model the pollution field by using only the data of a few stations; this is denoted as I-1. Here the emphasis of modeling is to construct the pollution field not only in the interpolation region, but also to extrapolate and predict the field in time. Pollutants are assumed to change slowly in time so that complete information about them is not used. Only the arguments from the stations data are included in the formulation.

1-1.

(i) for prediction

$$q_{i,j}^{t+1} = f_j(q_{i,j}^t, q_{i-1,j}^t, q_{i+1,j}^t, q_{i,j}^{t-1}, q_{i,j}^{t-2}, \cdots, q_{i,j}^{t-\tau},$$
$$q_{i,k}^t, q_{i-1,k}^t, q_{i+1,k}^t, q_{i,k}^{t-1}, q_{i,k}^{t-2}, \cdots, q_{i,k}^{t-\tau}); \tag{4.35}$$

(ii) for extrapolation

$$q_{i+1,j}^t = f_j(q_{i,j}^t, q_{i,j}^{t-1}, q_{i,j}^{t+1}, q_{i-1,j}^t, q_{i-2,j}^t, \cdots, q_{i-\tau,j}^t,$$
$$q_{i,k}^t, q_{i,k}^{t-1}, q_{i-1,k}^t, q_{i,k}^{t+1}, q_{i-2,k}^t, \cdots, q_{i-\tau,k}^t), \tag{4.36}$$

where $q_{i,j}^t$ is the pollution parameter j measured at the station i at the time t; f_j indicates the vector of polynomial functions corresponding to j parameters. The input variables may include delayed and higher-ordered arguments; for example, q_j^{t-1}, q_k^{t-1}, $\cdots$, q_j^2, q_k^2, $\cdots$, $(q_j^t q_k^t)$, $(q_j^t q_j^{t-1})$, $\cdots$ at station i.

   One can encounter the influence of the phenomena considering the settling of polluting particles. External influences with the above diffusion process and source function are

introduced. The source function includes perturbations such as the wind force vector P and its projection on x−axis V'. In general, the formulation for prediction looks like

$$q_{i,j}^{t+1} = f_j(\cdots) + f(x, t) + Q(P, V'), \tag{4.37}$$

where $f(x, t)$ is the trend function with the coordinates of x and t is the pollution component; similarly one can write for the extrapolation.

The second problem is formulated to model the physical field by using the "input-output matrix" along with the above turbulant diffusion equations. This is usually recommended when forecasting of the pollution changes in time. This has three formulations; these are denoted by II-1, II-2, and II-3 as given below.

II-1. In the first formulation, the "input-output matrix" uses only information from the stations. The prediction equation at the station i is

$$q_{i,j}^{t+1} = \sum_{s=1; s \neq i}^{n} f_{s,j}(q_s), \tag{4.38}$$

where q_s denotes the vector of $[q_{s,1}^t, q_{s,1}^{t-1}, \cdots, q_{s,1}^{t-\tau}, \cdots, q_{s,j}^t, q_{s,j}^{t-1}, \cdots, q_{s,j}^{t-\tau}]$; $j = 1, \cdots, m$ are pollution parameters; n is number of stations; $/$ is a polynomial function operator; m is the number of components. The pollution at the rth station (or field point) depends on the values measured at the neighboring points. For example, $n = 3$, $m = 2$, and $T = 2$

$$q_{1,1}^{t+1} = f_{2,1}(q_{2,1}^t, q_{2,1}^{t-1}, q_{2,1}^{t-2}, q_{2,2}^t, q_{2,2}^{t-1}, q_{2,2}^{t-2}) + f_{3,1}(q_{3,1}^t, q_{3,1}^{t-1}, q_{3,1}^{t-2}, q_{3,2}^t, q_{3,2}^{t-1}, q_{3,2}^{t-2}). \tag{4.39}$$

II-2. In the second formulation, it uses the "input-output matrix" containing only information about the pollutants. The prediction equation for station i is

$$q_{i,j}^{t+1} = \sum_{s=1}^{p} f_{s,j}(u_s), \tag{4.40}$$

where u_s denotes the vector of pollutants $[u_{s,1}^t, u_{s,1}^{t-1}, \cdots, u_{s,1}^{t-\tau}, \cdots, u_{s,m}^t, u_{s,m}^{t-1}, \cdots, u_{s,m}^{t-\tau}]$; P is the number of sources. For example, $m = 2$, $r = 2$, and $p = 2$

$$q_{1,1}^{t+1} = f_{1,1}(u_{1,1}^t, u_{1,1}^{t-1}, u_{1,1}^{t-2}, u_{1,2}^t, u_{1,2}^{t-1}, u_{1,2}^{t-2}) + f_{2,1}(u_{2,1}^t, u_{2,1}^{t-1}, u_{2,1}^{t-2}, u_{2,2}^t, u_{2,2}^{t-1}, u_{2,2}^{t-2}). \tag{4.41}$$

II-3. In the third formulation, it uses the "input-output matrix" containing the information of neighboring stations and the pollution sources—both q and u appear in the matrix. The prediction for station i is

$$q_{i,j}^{t+1} = \sum_{s=1; s \neq i}^{n} f_{s,j}(q_s) + \sum_{s=1}^{p} f_{s,j}(u_s). \tag{4.42}$$

It is good practice to add a source function Q to the above formulations in order to consider external influences like wind force, temperature, and humidity. The complete descriptions are obtained as sums of polynomials as was the case in the first problem. The formulations with the source function may also be considered for multiplicative case; for example,

$$q_{t+1} = Q_1(P, V') + Q_2(P, V')\left[\sum_{s=1; s \neq i}^{n} f_{s,j}(q_s) + \sum_{s=1}^{p} f_{s,j}(u_s)\right]. \tag{4.43}$$

This is done if it provides a deeper minimum of the external criterion.

The third problem is formulated to model the pollution field by using the principles of "close action" and "remote action." This has three formulations.

III-1. This uses the "close action" principle as well as information of stations forming the "input-output matrix;" this means that a combination of I-1 and II-1 is used in its formulation.

III-2. This uses the "principle of close action" and information of pollutants forming the "input-output matrix;" thus, a combination of I-1 and II-2 is used in its formulation.

III-3. This uses the "principle of close action" and information of stations and sources of pollutions from the extended "input-output matrix;" this means that a combination of I-1 and II-3 is used in its formulation.

The above seven types of formulations are synthesized and compared for their extrapolations and predictions by using a simulated physical field. The field is constructed using a known deterministic formula that allows changes of pollution without wind and that assumes that particles diffusion in space.

$$q = \frac{2\pi R}{kx} \int_{x=\frac{R}{kt}}^{\infty} \frac{e^{-x}}{x} dx, \tag{4.44}$$

where k is the turbulant diffusion coefficient, R is the distance between station and source, and t is time from the start of pollution to the time of measuring. The number of sources is assumed to be one. The change of pollution source and concentration of polluting substances are shown in Figure 4.5; the above formula is used to obtain the data. Integral values serve as the arguments.

All polynomials are evaluated by the combined criterion c3, "bias plus prediction error."

$$c3^2 = \bar{\eta}_{bs}^2 + \bar{i}^2(W), \tag{4.45}$$

where $\bar{\eta}_{bs}^2$ and $\bar{i}^2(W)$ are the normalized minimum bias and prediction criteria, respectively. For extrapolation error $\bar{\Delta}^2(C)$ is used instead of step-by-step prediction errors.

$$\eta_{bs}^2 = \frac{\sum_{p=1}^{\delta N_W}(\hat{q}_p^A - q_p)(\hat{q}_p^B - q_p)}{\sum_{p=1}^{\delta N_W} q_p^2}, \tag{4.46}$$

where 6 is the noise immune coefficient that varies from 1.5 to 3.0, and

$$i^2(W) = \frac{\sum_{p \in N_W}(\hat{q}_p - q_p)^2}{\sum_{p \in N_W} q_p^2}. \tag{4.47}$$

The solutions of the first and second problems allow one to construct the field, extrapolate, and predict along the spatial coordinates. The solution of the second problem also allows one to interpolate, extrapolate, and predict pollution parameters at the stations. The results show that the model, based on the "principle of close action," cannot survive alone for better predictions compared with the model that are based on the "principle of remote action" (II-3) and on the "combined principle" (III-2).

Model II-3.

$$q_1^{t+1} = 2.0361 - 2.1815q_2^{t-1} - 0.2102q_2^{t-3} + 0.00754u^{t^2} + 0.1099q_2^t q_2^{t-2} + 0.3924q_2^{t-1}$$
$$+ 0.00002q_2^{t^2} - 0.000002q_2^t q_3^{t-1} - 0.000001q_3^{t^2}. \tag{4.48}$$
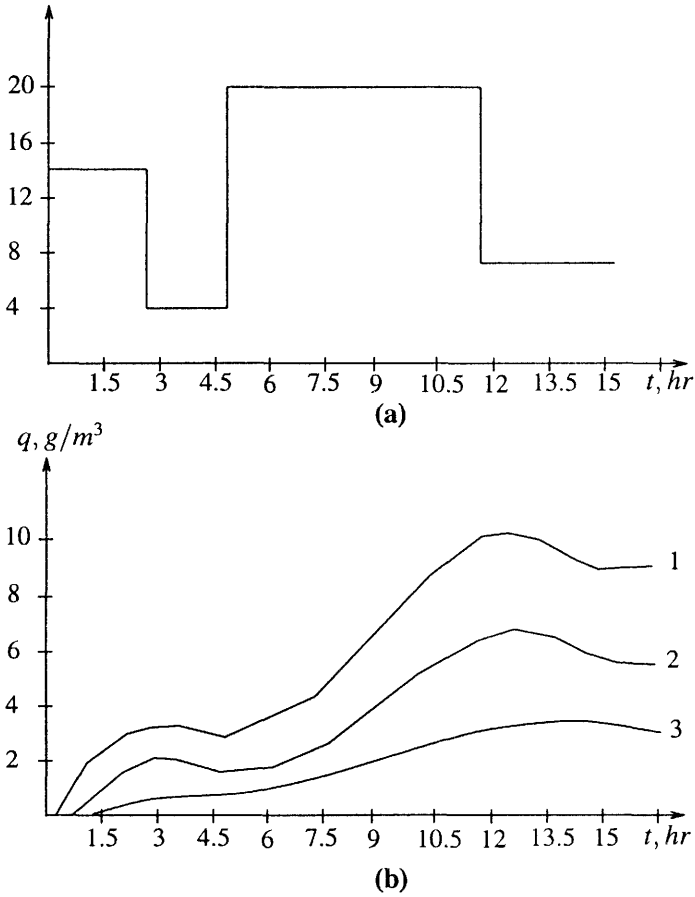
Figure 4.5.   (a) Change of pollution discharge in time (from the experiment) and (b) change in concentrations of polluting substances at stations 1, 2, 3.

Model III-2.

$$q_j^{t+1} = 0.4228 - 0.7792q_j^t - 0.5797q_j^{t-1} - 0.4908q_j^{t-3} + 0.94q_{j-1}^t + 1.1502q_{j+1}^t$$
$$+ 0.0442u_j^{t-2} + 0.0047q_j^{t^2} + 0.0017q_j^t q_j^{t-1} + 0.0018q_j^t q_j^{t-2} + 0.0074q_j^{t-1} q_j^{t-2}$$
$$- 0.0211q_j^{t-1} q_j^{t-3} + 0.0045q_j^{t-1} q_{j+1}^t - 0.0066q_j^{t-2} q_{j-1}^t - 0.0021q_j^{t-2} q_{j+1}^t$$
$$+ 0.0187q_j^{t-3} q_{j-1}^t - 0.0032q_{j-1}^{t^2} - 0.002q_{j-1}^t q_{j+1}^t, \tag{4.49}$$

where j indicates the pollution component pertaining to the station 1.

Figures 4.6 to 4.8 illustrate the step-by-step predictions of all formulations. Table 4.4 gives the performance of these formulations on the given external criteria.
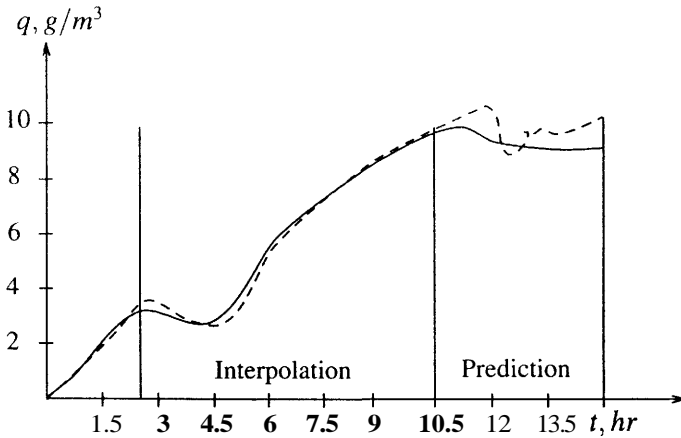
Figure 4.6. Performance of model I-1 ("close" action principle)

Table 4.4. Performance of the formulations

Formulation	c3	η_{bs}	$\Delta(C)$	i
I-1	0.032	0.017	0.027	0.182
II-1	0.061	0.046	0.040	0.188
II-2	0.089	0.082	0.036	0.169
II-3	0.080	0.054	0.059	0.151
III-1	0.064	0.063	0.026	0.176
III-2	0.033	0.009	0.031	0.149
III-3	0.115	0.050	0.040	0.246

3 CYCLIC PROCESSES

We have studied the formulations based on the "principle of continuity or close action," the "principle of distant or remote action," and, to some extent the "principle of combined action" using a combination of formulations. The "close action principle" is realized by considering nearby cells and delayed arguments in the finite-difference analogues. The "remote action principle" is arrived at by constructing the "input-output matrix," which is one way of realizing this principle. The elements in the "input-output matrix" can be the values of perturbations or values of variables in distant cells. The "combined action" gives the way to consider the influence of both principles on the output variable.

Many processes in nature that have characteristic cyclic or seasonal trend are oscillatory. For example, the mean monthly air temperature has characteristic maxima during the summer months and minima during the winter months. These values of maxima and minima do not coincide with one another from year to another. Therefore, processes with seasonal fluctuations of this kind are called cyclic in contrast with the strictly periodic processes. They include all natural processes with constant duration—a cycle (year or day). The variations in these processes are determined by the influence of supplementary factors. Certain agricultural productions, economical processes (sale of seasonal goods, etc.), and technological processes might be classified as cyclic. These are described by integro-differential
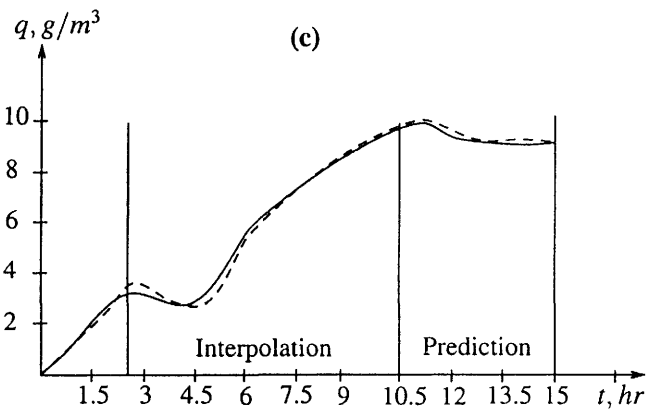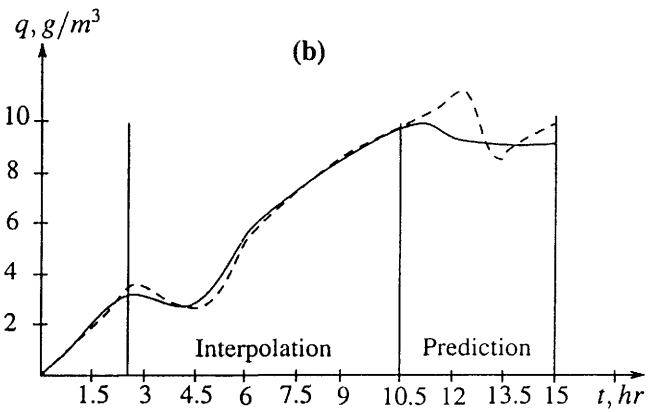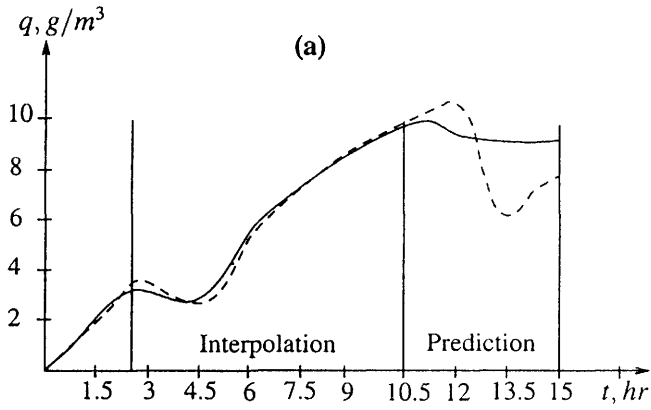
Figure 4.7. Performance of (a) model II-1, (b) model II-2, and (c) model II-3 for "remote" action principle
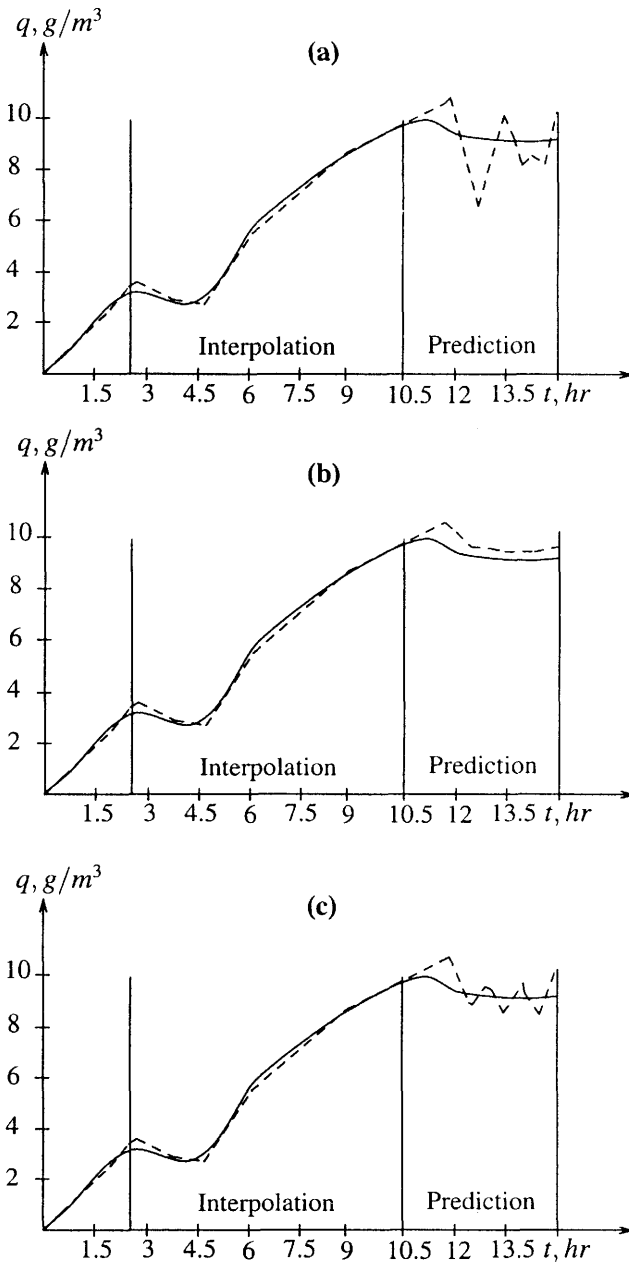
Figure 4.8. Performances of (a) model III-1, (b) model III-2, and (c) model III-3 for "close" and "remote" action principles

equations—among such processes are the non-Markov processes. Such equations contain terms such as moving averages (sometimes referred to as "summation patterns"). For example, an equation of the form

$$\int_{t_k}^{0} q dt + \frac{dq}{dt} + q = 0 \qquad (4.50)$$

has a finite-difference analogue as

$$a_1 \frac{1}{k+1}(q^{t-k} + \cdots + q^{t-1} + q^t) + a_2(q^t - q^{t-1}) + a_3 q^t = 0. \qquad (4.51)$$

The "summation pattern" represents the moving average of k cells in the interval of integration. In training the system, the moving averages take place along with the other arguments of the model. For each position of the pattern on the time-axis, corresponding summation patterns are considered.

The use of summation patterns for obtaining predictive models implies a change from the principle of close- or short-range action to the principle of combined action because the general pattern of the finite-difference scheme is doubly connected. In other words, during self-organization modeling, two patterns are used: one for predicting the output value and the other for the value of the sum. Predictive models have a single pattern that is based on the "principle of close action" are suitable only for short-range predictions. For example, weather forecasting for more than 15 days in advance using hydrodynamic equations (the principle of close action) is impossible.

Long-range predictions require a transfer to equations based on the principle of long-range action and combined models. In a specific sense, such models are a result of using the interior of balance of variables based on the combined principle. The external criterion that is based on a balance law allows specification of a point in the distant future, through which the integral curve of stepwise prediction passes, and selects the optimal prediction model. It enables overcoming the limit of prediction characteristic of the principle of short-range action.

The criterion of balance-of-variables (refer to Chapter 1) is the simplest way to find a definite relationship (a physical law) among several variables being simultaneously predicted. This is the basis of long-range prediction using the ring of "direct" and "inverse" functions. The ring can be applied both for algebraic and finite-difference equations. The second form of the balance-of-variables criterion is the prediction balance criterion, which fulfills the balance law. This simultaneously uses two or more predictions that differ in the interval of variable averaging in selecting the optimal model. For example, in choosing a system of monthly models the algorithm utilizes the sequence of applying the criteria

$$F_0 \rightarrow F_1(\eta_{bs}) \rightarrow F_2(B_{month}) \rightarrow F_3(B_{year}); \quad F_3 \ll F_2 \ll F_1 \ll F_0, \qquad (4.52)$$

where F_1 number of models are selected out of F_0 number of models using the minimum bias criterion η_{bs} or prediction criterion i—in the case of a small number of data points. Using the monthly balance criterion B_{month}, F_2 number of models are selected from F_1. Finally, using the annual balance, one optimal model or a few models (F_3) are chosen.

Here we describe the model formulations with one-dimensional and two-dimensional readout and the realization of the prediction balance criterion for cyclic processes.

3.1   Model formulations

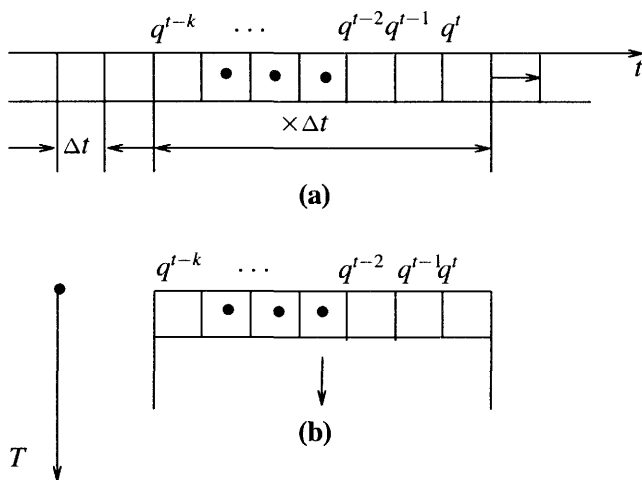One-dimensional and two-dimensional models are given for comparison.

Figure 4.9. Pattern movement. The arrow indicates movement during training along (a) a $t-$axis, and (b) a $T-$axis

One-dimensional time readout

Let us assume that given a sampled data, q^t is the output value at time t depending on its delayed values $q^{t-1}, q^{t-2}, \cdots$. We have

$$q^t = f_1(t) + f_2(q^{t-1}, q^{t-2}, q^{t-3}, \cdots), \tag{4.53}$$

where f_1 is the source function, which is a trend equation as $q^t = f_1(t)$. The data, given in discrete form, is designated at equal intervals of time (Figure 4.9).

Two-dimensional time readout

If the process has an apparent repetitive (seasonal, monthly) cycle, one can also apply a two-dimensional readout. For example, let t be time measured in months and T the time measured in years. The experimental data takes the shape of a rectangular grid (Figure 4.10). The model includes the delayed arguments from both the monthly and yearly dimensions in the two-dimensional fields,

$$q_{t,T} = f_1(t, T) + f_2(q_{t-1,T}, q_{t-2,T}, \cdots, q_{t,T-1}, q_{t,T-2}, \cdots), \tag{4.54}$$

where $f_1(t, T)$ is the two-dimensional "source function"—considered two-dimensional time trend equation.

The trend functions are obtained through self-organization modeling by using the minimum bias criterion. With the one-dimensional time readout, the training of the data is carried out using its transposition along the horizontal axis t. With the two-dimensional time readout, training is done by transposing the pattern along the vertical axis T (Figure 4.11) for individual columnwise models or along the both axes (t, T) for a single model. Connecting the participating delayed arguments of the output variable provides the shape of the pattern used in the formulation.

One advantage with the data of two-dimensional time readout is that it can be used to build up a system of equations (the seasonal fluctuations in the data are taken care of by
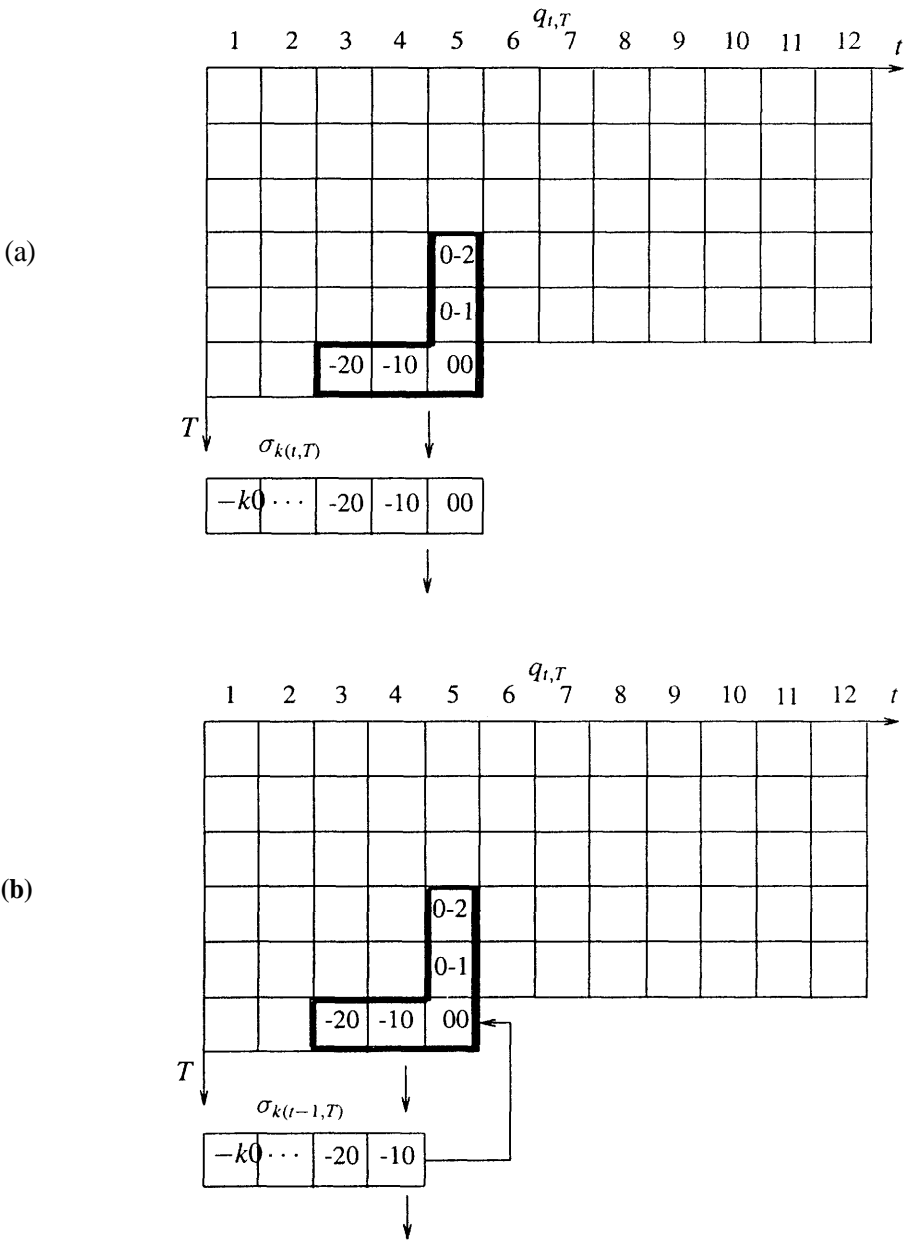
Figure 4.10. Scheme for two-dimensional time readout: (a) a model using predictions of moving averages $\sigma_{k(t,T)}$ and (b) a model using the averages $\sigma_{k(t-1,T)}$ as arguments.
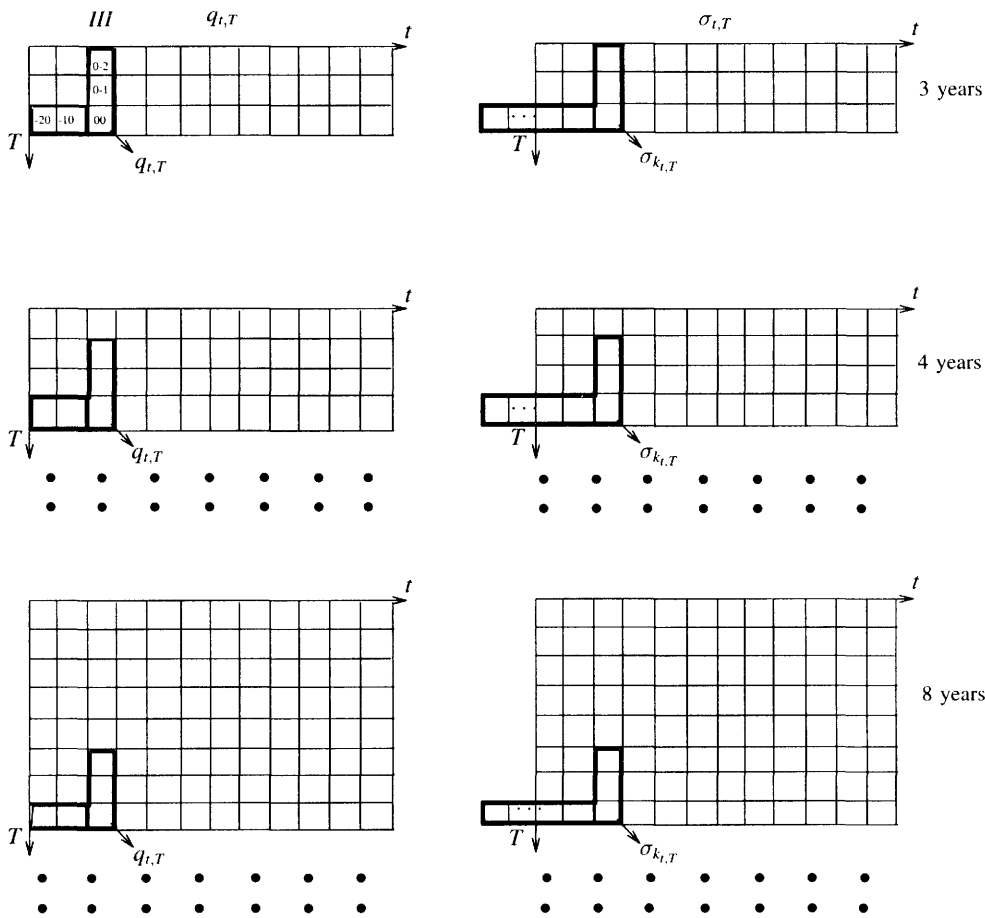
Figure 4.11. Schematic diagram for training of the model for the month of March by transposing patterns $q_{t,T}$ and $\sigma_{k_{(t,T)}}$ along the $T-$ axis.

the system of equations). Each model in the system of equations is valid only for the given month and the system of equations (twelve monthly models) for the whole process. For a long-range prediction with stepwise integration, a transition is realized from one month''s model to the next month's model. Similarly, the idea of three-dimensional time readout can be realized in modeling cyclic processes (for example, period of solar activity; see Figure 4.12).

Moving averages   In modeling of cyclic processes, one or more of the following moving averages are considered arguments of the model [65].

$$\sigma_{k_{t,T}} = \frac{1}{k}(q_{t,T} + \cdots + q_{t-(k-1),T}); \quad k = 2, 3, \cdots, 12 \tag{4.55}$$

When one moving average is used, it is reasonable to select precisely that moving average which ensures the deepest minimum to the model. If all possible moving averages are used, there remain only the most significant ones—usually two averages σ_3 and σ_{12} corresponding to season and year remain more frequently than others. Moving averages can also be considered by giving weights to the individual elements.
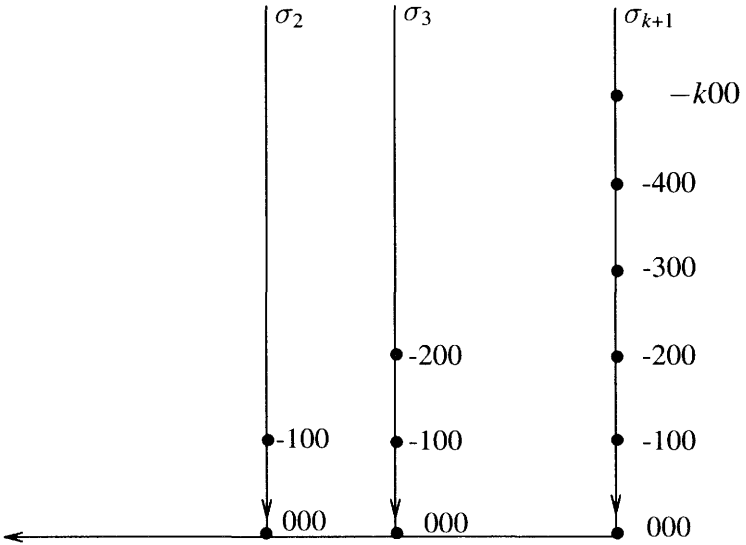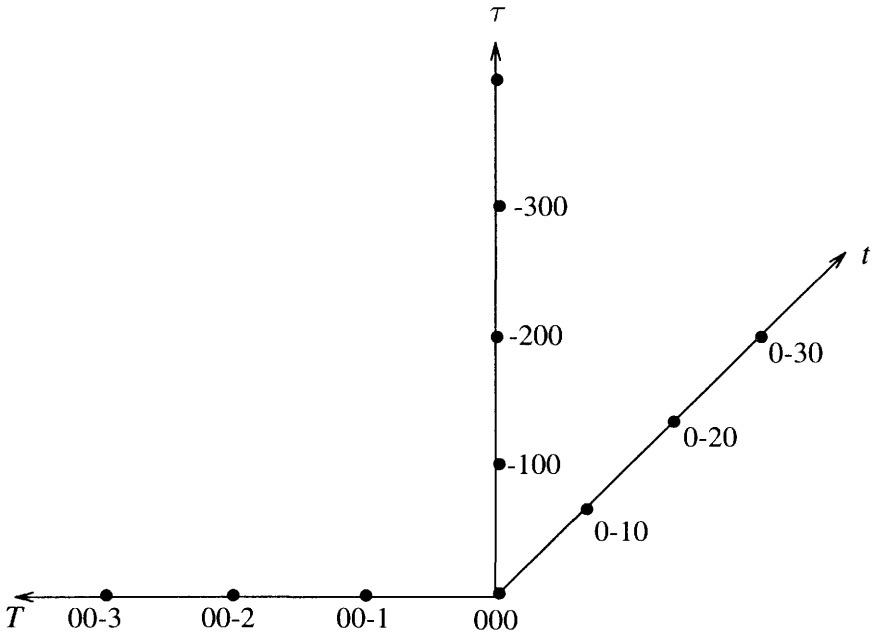
Figure 4.12. Pattern representation for three-dimensional time readout, where t represents months, T years, and τ units of 11.2 years (in case of solar activity).

Monthly models

In the two-dimensional time readout, each cell of the numeric grid (t, T) is represented through the output value q and the estimated value of a moving average σ_k. For example, a monthly prediction model has the form

$$q_{t,T} = f_1(t, T) + f_2(q_{t-1,T}, q_{t-2,T}, \cdots, q_{t,T-1}, q_{t,T-2}, \cdots,$$

$$\hat{\sigma}_{k_{t,T}}, \sigma_{k_{t-1,T}}, \sigma_{k_{t-2,T}}, \cdots, \sigma_{k_{t,T-1}}, \sigma_{k_{t,T-2}}, \cdots). \tag{4.56}$$

The estimated values $q_{t,T}$ and $\sigma_{k_{t,T}}$ are not known in the process of prediction, but the others can be determined from the initial data or by predictions. The monthly prediction model (full description) for $\sigma_{k_{t,T}}$ is

$$\hat{\sigma}_{k_{t,T}} = f_3(t, T) + f_4(\hat{q}_{t,T}, q_{t-1,T}, q_{t-2,T}, \cdots, q_{t,T-1}, q_{t,T-2}, \cdots), \tag{4.57}$$

where f_1, f_2, f_3, and f_4 are the polynomials. There are auxiliary variables that can be used in the complete descriptions.

3.2   Realization of prediction balance

The balance relation b for the prediction of sth year is expressed by

$$b_s = [\hat{\sigma}_{k_{t,T}}]_s - \frac{1}{k+1}(\hat{q}_{t,T} + q_{t-1,T} + q_{t-2,T} + \cdots + q_{t-k,T})_s, \tag{4.58}$$

where $s = 1, 2, \cdots, N$ and N is the number of years of observing process. The criterion of monthly prediction balance for each month is written as

$$B_{month} = \sum_{s=1}^{N} b_s^2. \tag{4.59}$$

It is difficult to see the feasibility of the criterion in this form because we need to know $\sigma_{k_{tT}}$ to predict $q_{t,T}$. We need to know $q_{t,T}$ to predict $\sigma_{k_{t,T}}$. This requires a recursive procedure. Assuming the initial value $q_{t,T}$- 0, we find $\sigma_{k_{t,T}}$, the second value $q_{t,T}$, and so on until the value of the criterion B_{month} decreases. It is necessary to eliminate either $\sigma_{k_{tT}}$ or $q_{t,T}$ from the composition of the arguments. (Possible simplification follows below.)

The monthly prediction model for q is

$$\hat{q}_{t,T} = \hat{\sigma}_{1_{t,T}} = f_1(t, T) + f_2(\hat{\sigma}_{k_{t,T}}, \sigma_{k_{t-1,T}}, \sigma_{k_{t-2,T}}, \cdots, \sigma_{k_{t,T-1}}, \sigma_{k_{t,T-2}}, \cdots,$$

$$q_{t-1,T}, q_{t-2,T}, \cdots, q_{t,T-1}, q_{t,T-2}, \cdots). \tag{4.60}$$

The monthly prediction model for σ_k is

$$\hat{\sigma}_{k_{t,T}} = f_3(t, T) + f_4(q_{t-1,T}, q_{t-2,T}, \cdots, q_{t,T-1}, q_{t,T-2}, \cdots,$$

$$\sigma_{k_{t-1,T}}, \sigma_{k_{t-2,T}}, \cdots, \sigma_{k_{t,T-1}}, \sigma_{k_{t,T-2}}, \cdots). \tag{4.61}$$

The criterion of monthly balance remains unchanged and is in usable form with the simplification in the formulations.

$$B_{month} = \sum_{i=3}^{N} b_i^2. \tag{4.62}$$

The sequential application of criteria is according to the scheme $F_0 \rightarrow F_1(\eta_{bs}) \rightarrow F_2(B_{month}) \rightarrow F_3(B_{year})$.

The patterns of the above models are doubly connected (Figure 4.10). One can use the expanded set of arguments and can also eliminate the predicted value of $\sigma_{k_t,T}$. One can use the combined criterion of "minimum bias plus prediction" in place of minimum bias criterion. When a small number of data points are used, minimum bias criterion can be replaced by the prediction criterion for step-by-step predictions of A months ahead.

$$i^2(\lambda) = \frac{\sum_{k=1}^{\lambda}(q_k - \hat{q}_k)^2}{\sum_{k=1}^{\lambda} q_k^2}$$

$$I^2(\lambda) = \frac{1}{N} \sum_{s=1}^{N}[i^2(\lambda)]_s. \tag{4.63}$$

For example, let us assume that A = 3. To select models for the month of March, one must obtain all possible models for March, April, and May. The predictions of these models are used sequentially in computing the prediction criterion error. To obtain the data, the patterns are used along the t, T-coordinate field as indicated in Figure 4.11.

$$[i^2(3)]_s = [\frac{\sum_{i=III}^{V}(q_i - \hat{q}_i)^2}{\sum_{i=III}^{V} q_i^2}]_s$$

$$I^2(3) = \frac{1}{N} \sum_{s=1}^{N}[i^2(3)]_s. \tag{4.64}$$

The criterion $I(3)$ demands that the average error in predictions that consider a three-month model should be minimal. This determines the optimal March model; F_1 number of March models are selected. Usually F_1 is not greater than two to three models.

The criterion of yearly balance is used in selecting all 12 models; one model for each month is selected such that the system of 12 models would give the maximum assurance of the most precise prediction for the year.

$$B_{year}^2 = \frac{1}{N} \sum_{s=1}^{N}[\bar{q}_{year} - \frac{1}{12}(\hat{q}_I + \hat{q}_{II} + \cdots + \hat{q}_{XII})]_s^2, \tag{4.65}$$

where q_{year} is the average yearly value computed directly and used in training. The predictions $(\hat{\bar{q}}_{year})$ can be obtained by using a separate algorithm, such as a harmonic algorithm, while the B_{year} is calculated.

Various sequences of applying criteria can be written as

$$F_0 \rightarrow F_1(\eta_{bs}) \rightarrow F_2(B_{month}) \rightarrow 1(B_{year}),$$
$$F_0 \rightarrow F_1(c3) \rightarrow F_2(B_{month}) \rightarrow 1(B_{year}),$$
$$F_0 \rightarrow F_1[I(\lambda)] \rightarrow F_3(B_{year}),$$
$$F_0 \rightarrow F_1(c3) \rightarrow F_3(B_{year}), \tag{4.66}$$

and so on. The selection of sequence differs in a number of ways depending on the mathematical formulation, availability of data, and user's choice.

3.3 Example—Modeling of tea crop productions

Example 5.   Modeling of a cyclic process such as tea crop production is considered here [59], [87].

First we give a brief description of the system. The cultivation of tea on a large scale is only about 100 years old. North Indian tea crop production accounts for 5/6 percent of the country's tea output. Tea is cultivated in nearly all the subtropics and mountainous regions of the tropics. When dormant, the tea shrub withstands temperatures considerably below freezing point, but the northern and southern limits for profitable tea culture are set by the freezing point. A well-distributed annual rain fall of 150 to 250 cms. is good for satisfactory growth. Well drained, deep friable loam or forest land rich in organic matter is ideal for growing the tea crop. Indian tea soils are low in lime content and therefore somewhat acidic. The subsoil should not be hard or stiff. The fertilizer mixtures of 27 kg. of N, 14 kg. of P_2O_5 and 14 kg. of K_2O per acre are applied in one or two doses.

In North India tea leaves are plucked at intervals of seven to ten days from April to December; whereas in the South plucking is done throughout the year at weekly intervals during March to May (the peak season) and at intervals of 10 to 14 days during other months. The average yield per acre is about 230 to 280 kg. of processed tea. Vegetatively propagated clones often give as much as 910 kg. of tea per acre. The quality of tea depends not only on the soil and the elevation at which the plant is grown, but also on the care taken during its cultivation and processing.

Here two cases are considered: one for modeling of North Indian tea crop productions and another for South Indian tea crop productions. The weather variables, such as mean monthly sunshine hours, mean monthly rain fall, and mean monthly water evaporation (data collected from the meteorological stations during the same period), can be used in the modeling.

The following sets of variables are considered for the model formulations.

$$(t, T) \in \tau$$
$$(q_{t-1,T}, q_{t-2,T}, \cdots, q_{t,T-1}, q_{t,T-2}, \cdots) \in \mathcal{P}$$
$$(\sigma_{2_{t-1,T}}, \sigma_{3_{t-2,T}}, \cdots, \sigma_{12_{t-1,T}}) \in \sigma$$
$$(S_{t,T}, S_{t-1,T}, S_{t-2,T}, \cdots, S_{t,T-1}, S_{t,T-2}, \cdots,$$
$$R_{t,T}, R_{t-1,T}, R_{t-2,T}, \cdots, R_{t,T-1}, R_{t,T-2}, \cdots,$$
$$E_{t,T}, E_{t-1,T}, E_{t-2,T}, \cdots, E_{t,T-1}, E_{t,T-2}, \cdots) \in \mathcal{Z}, \tag{4.67}$$

where t and T are the time coordinates measured in months and years, respectively; $q_{t,T}$ is considered the output variable measured at the coordinates of $(t, 7)$; $q_{t-i,T}$ and $q_{t,T-j}$ are the delayed arguments at i units in months and j units in years, correspondingly; $\sigma_{k_{t-1}T}$ - $\frac{1}{k}(q_{t-1,T} + q_{t-2,T} + \cdots + q_{t-k,T})$ are the moving averages of length k. The weather variables $S, R,$ and E represent sunshine hours, rainfall, and water evaporation, correspondingly.

In modeling North Indian tea crop productions the following model formulation is adopted for each month.

7-7.

$$q_{t,T} = f(\mathcal{P}, \sigma). \tag{4.68}$$

Because of a small number of data points, the complete polynomial below is used as reference function for each month.

$$q_{t,T} = a_0 + a_1 q_{t-1,T} + a_2 q_{t,T-1} + a_3 \sigma_{3_{t-1}T} + \text{fl4cr6}, \_,_T. \tag{4.69}$$

The sequence of criteria, which has shown better performance than other sequences, is shown here.

$$F_0 \rightarrow F_1(\eta_{bs}) \rightarrow F_2[I(3)] \rightarrow 1(B_{year}). \tag{4.70}$$

The total number of data points correspond to eleven years; $N_A = 5, N_B = 5$, and $N_C = 1$. The coefficient values of the best system of monthly models are given as

Month i	a_0	fli	a_2	a_3	a_4
1	0.318	0.026	-0.366		
2	-0.010	0.022	-0.384	0.013	
3	-6.730				0.452
4	-0.620		-0.084		1.309
5	0.276	-1.040			4.335
6	35.350	-0.820	-0.174	2.289	
7	18.010		0.321		1.227
8	67.730	-1.124		-1.459	4.571
9	18.110	0.313			0.576
10	-10.340	1.110			
11	-23.850	-1.017	-0.293		2.485
12	-10.530			3.498	-2.933

 The blank spaces indicate that the corresponding variable does not participated in the model. The prediction error on the final-year data is computed as 0.0616. The system of monthly models is checked for stability in a long-range perspective.

    In modeling South Indian tea crop productions, five types of model formulations are considered as complete polynomials that are studied independently.

Different formulations

II-1.

$$q_{t,T} = f(\tau, \mathcal{P}, \sigma, \mathcal{Z}), \tag{4.71}$$

where / is a single function that considers all variables. It is considered a one-dimensional model that represents the system.

77-2.

$$q_{t,T} = f_1(\tau) + f_2(\mathcal{P}, \sigma, \mathcal{Z}), \tag{4.72}$$

where f_1 is the trend function in two time coordinates; f_2 is the function of delayed arguments, moving averages, and other input variables. Use of the two-dimensional time trend function is preferred when the initial data is noiseless and when individual components of the cyclic processes that have a character of time variation have no effect. The behavior of f_2 is supposed to be effected by these variables.

    This formulation is evaluated in two levels. First, the trend function is estimated based on whole data, residuals are computed, and the function f_2 is estimated using the residuals. The final prediction formulation will be the summation of both.

77-3.

$$q_{t,T} = f_i(\tau, \mathcal{P}, \sigma); \quad i = 1, 2, \cdots, 12. \tag{4.73}$$

This is similar to the formulation II-1, but represents the system of 12 monthly models; 12 separate prediction formulas f_i for each month.
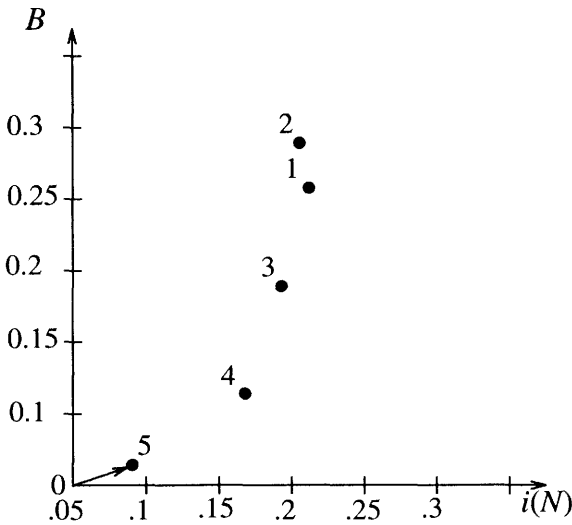
Figure 4.13.   Selection of optimal model on two criterion analysis

II-4.

$$q_{t,T} = f_1(\tau) + f_{2_i}(\mathcal{P}, \sigma); \quad i = 1, 2, \cdots, 12. \tag{4.74}$$

This is similar to the formulation II-2, but has a system of 12 monthly models at the second level. The trend function f_1 is a single formula, as in the formulation II-2. The residuals are computed on all data; this data is used for identifying the system of 12 monthly models f_{2_i}.

II-5.

$$q_{t,T} = f_{1_i}(\tau) + f_{2_j}(\mathcal{P}, \sigma); \quad i, j = 1, 2, \cdots, 12. \tag{4.75}$$

Time-trend equations for each month are separately identified; in other words, the function $f_{1_i}(\tau)$ is considered a function of T for each month. The residuals are computed and the second set f_{2_j} of the system of monthly models are obtained. This makes a set of combined models for me system.

Each formulation is formed for its complete polynomial; combinatorial algorithm is used in each case for sorting all possible combinations of partial polynomials as "structure of functions." The optimal models obtained from each case are compared further for their performance in predictions. The scheme of the selection criteria is

$$F_0 \rightarrow F_1(c3) \rightarrow F_2[i(N)] \rightarrow 1(B_{year}), \tag{4.76}$$

where c3 is the combined criterion with "minimum bias (η_{bs}) plus prediction $(i(W))$," $i(W)$ being the prediction criterion used for step-by-step predictions on the set W, and $i(N)$—the whole data set N.

The data used in this case belong to ten years; $N_A = 4$, $N_B = 4$, and two years data is preserved for checking the models in the prediction region. The simplest possible pattern is considered for the formulations II-3, II-4, and II-5, because of the availability of a few collected data. In the monthly models the weather variables are not considered for simplicity. One can see the influence of such external variables in the analysis of cyclic processes. All
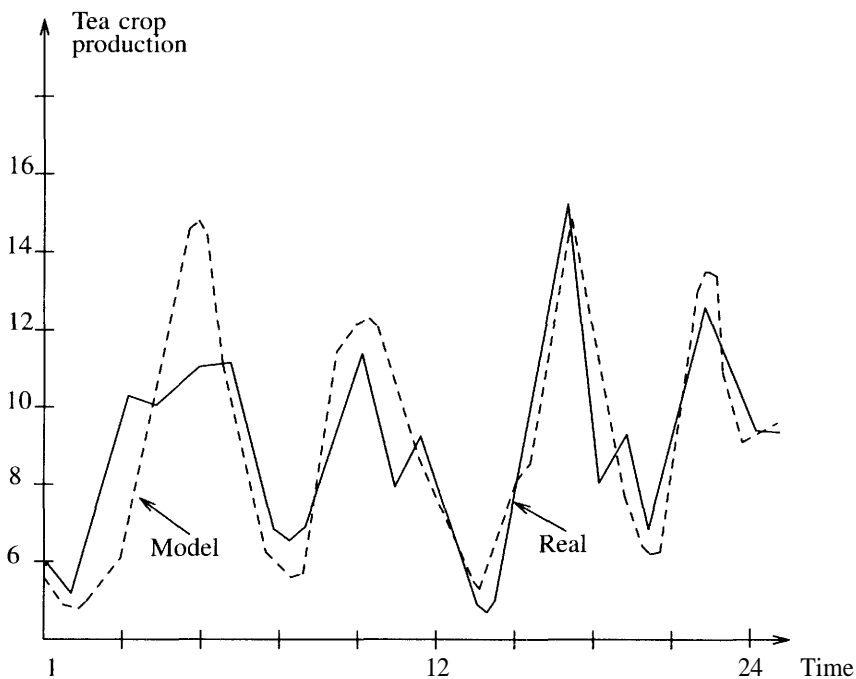
Figure 4.14. Performance of the best model

optimal models are compared for their step-by-step predictions of up to ten years and tested for their stability in long-range actions. The results indicate that the formulation II-5 has optimal ability in characterizing the stable prdictions (shown in Figures 4.13 and 4.14). The system of monthly models in an optimum case is given below; first, the set of time trend models is

$$f_{1_i}(T) = a_0 + a_1 T + a_2 T^2 + a_3 T^3 + a_4 T^4, \qquad (4.77)$$

where

Month i	a_0	a_1	a_2	a_3	a_4
1	5.801	0.048			
2	12.380	-1.587	0.070	-0.006	
3	6.289			-.000012	
4	9.454	-0.082			
5	10.364	0.368			
6	8.141	0.937	-.070		
7	6.009	0.057			
8	5.665	0.076			
9	7.678	0.316	-.013		
10	6.588	1.917	-.258		
11	6.288			-.000012	
12	5.659	0.076			

and the set of remainder models is

$$f_{2_i}(\mathcal{P}, \sigma) = b_1 q_{t-1,T} + b_2 q_{t,T-1} + b_3 \sigma_{3_{t-1,T}} + b_4 \sigma_{12_{t-1,T}}, \qquad (4.78)$$

where

Month i	b_1	b_2	b_3	b_4
1	0.626		-0.317	-0.260
2	0.168		-0.923	0.292
3	1.489		-1.501	-2.611
4	-0.774		-1.976	3.481
5	1.189		-2.196	1.215
6	-0.514		3.176	-1.588
7	-0.162		-0.647	1.188
8	0.355		0.109	-0.587
9	0.334	-0.034		-0.190
10	-0.298	-0.039		0.132
11	1.630		0.931	-3.238
12	-0.069			0.205

The blank space indicates that the corresponding variable does not participate in the monthly model. These two sets of monthly model systems form the optimal model for an overall system.

1-2 & II-6. Here is another idea for forming a model formulation which is not discussed above. This considers a harmonical trend at the first level instead of time trend.

$$q_{t,T} = f_1(\sin wt, \cos wt) + f_{2_i}(\mathcal{P}, \sigma, \mathcal{Z}), \qquad (4.79)$$

where f_1 represents a single harmonic function for the whole process with the arbitrary frequencies and f_{2_i} is the system of monthly models. At the first level the harmonic trend is obtained as $q_t = f_1(\sin wt, \cos wt)$ using the harmonical inductive algorithm. Residuals ($\Delta q_t = q_t - \hat{q}_t$) are computed using the harmonic trend, then the system of monthly models are estimated as in the above cases.

The first level of operation for obtaining the harmonical trend of tea crop productions is shown. The data q, is considered a time series data of mean monthly tea crop productions. The function f_1 is the sum of m harmonic components with pairwise distinct frequencies w_k, $k = 1, 2, \cdots, m$.

$$f_1 = \sum_{k=1}^{m}(A_k \sin w_k t + B_k \cos w_k t), \qquad (4.80)$$

where $w_i \neq w_j$, $i \neq j$; $0 < w_k < \pi$, $k = 1, 2, \cdots, m$. The function is defined by its values in the interval of data length N ($1 < t < N$).

The initial data is divided into training N_A, testing N_B, and examining N_C points. The maximum number of harmonics is $m_{max} lN/3$ ($1 < m < m_{max}$). The sorting of the partial trends that are formed based on the combination of harmonics is done by the multilayer selection of trends. In the first layer, the freedom of choice F best harmonics are obtained by the selection criterion on the basis of the testing sequence, the remainders are then calculated. In the second layer, the procedure is continued using the data of remainders and is repeated in all subsequent layers. Finally F best harmonics are selected. The complexity of the trends increases as long as the value of the "inbalance" decreases (refer to Chapter 2 for details on the harmonic algorithm). In the last layer, the unique solution corresponding to the minimum of the criterion is selected. As this algorithm is based on the data of remainders, the sifting of harmonics can be stopped usually at the second or third layer.

The data is separated into $NA = 90\%$, NB - 6%, and $NC = 4\%$, and m_{max} is considered as eight in these cases.

In North Indian tea crop productions model, the structure of the optimal harmonic trend is obtained as

$$\hat{q}_t = \sum_{i=1}^{l} \sum_{j=1}^{m_i} (A_{ij} \sin w_{ij}t + B_{ij} \cos w_{ij}t), \qquad (4.81)$$

where q_t is the estimated output, l is the number of layers, m_i are the number of harmonic components at each layer, and the parameters for $l = 3$ are given as

Layer	Components	Frequency	Coefficients	
i	m_i	w_{ij}	A_{ij}	B_{ij}
1	1	0.523	-24.64	-13.09
		0.693	-0.64	0.23
		1.052	-1.24	-2.13
		1.570	-0.60	-2.50
		1.988	0.28	-0.08
		2.285	-0.63	0.16
		2.775	0.53	-0.13
2	\	4.598	0.20	0.18
3	6	0.458	-0.68	0.69
		0.917	-0.37	0.07
		1.278	-0.32	0.16
		1.847	-0.15	0.82
		2.203	-0.12	0.22
		2.699	-0.21	-0.23

The root mean square (RMS) error on overall data is achieved as 0.0943.

In South Indian tea crop productions modeling, the data is initially smoothed to reduce the effect of noise by taking moving averages as

$$\bar{q}_t = \frac{1}{L} \sum_{k=1}^{L} q_{t+k-1}. \qquad (4.82)$$

This transformation acts as a filter that does not change the spectral composition of the process, but changes only the amplitude relation of the harmonic components [130]. The harmonic trend for q_t can be written as

$$\bar{q}_t = \frac{1}{L} \sum_{k=1}^{L} \sum_{j=1}^{m} [A_j \sin w_j(t+k-1) + B_j \cos w_j(t+k-1)]. \qquad (4.83)$$

After simple transformations, this can be reduced to the form:

$$\bar{q}_t = \sum_{j=1}^{m} (\bar{A}_j \sin w_j t + \bar{B}_j \cos w_j t). \qquad (4.84)$$

The filtered data is used for obtaining the harmonic trend. For fixing the optimal smoothing interval, the length of the summation interval L was varied from one to ten. For $L < 3$, the algorithm was not effective. L_{opt} is achieved at 4 because it is not expedient to greatly increase the value of L (Table 4.5). The optimal harmonic components for $l = 3$ and $L = 4$ are listed as

$$\hat{\bar{q}}_t = \sum_{i=1}^{l} \sum_{j=1}^{m_i} (A_{ij} \sin w_{ij}t + B_{ij} \cos w_{ij}t), \qquad (4.85)$$

Table 4.5. Effect of smoothing interval on the noisy data

L	RMS error
3	0.06779
4	0.05579
5	0.07321
6	0.06375
7	0.06648
8	0.05730
9	0.05647
10	0.04957

where $\hat{q}_t$ is the estimated filtered output;

Layer	Components	Frequency	Coefficients	
i	m_i	w_{ij}	A_{ij}	B_{ij}
1	4	0.486	-0.25	0.70
		0.846	-0.01	0.08
		1.073	0.08	-0.38
		2.371	-0.002	0.001
2	5	0.282	0.002	0.33
		0.508	0.309	0.03
		0.721	-0.26	0.04
		1.016	0.11	0.32
		1.193	-0.005	-0.03
3	3	0.452	0.41	-0.21
		0.853	0.03	-0.01
		1.236	-0.03	0.05

The RMS error on the filtered data is achieved as 0.05579. Part of the prediction results are shown in Figure 4.15.

3.4 Example—Modeling of maximum applicable frequency (MAF)

Example 6. Modeling of maximum applicable frequency (MAF) of the reflecting iono-spheric layer [43].

This example shows the applicability of self-organization method using the two-level prediction balance criterion for constructing short-range hourly forecasting models for the process of MAF variations at a preassigned point of the reflecting ionospheric layer. The general formulation of the models for the process of MAF variations can be set down as follows:

$$q^{t+1} = f(q^{t-\tau}, t) \tag{4.86}$$
$$q^{t+1} = f(q^{t-\tau}, t, u), \tag{4.87}$$

where q^{t+1} is the MAF value at the time $t + 1$ in MHz; $q^{t-\tau}$ is the delayed argument of q at the time $t - \tau$; t is the time of the day and u is the vector of the external perturbations. The size of the MAF is influenced by a large number of external perturbations, such as solar activity, agitation of the geomagnetic field, interplanetary magnetic field, cosmic rays, and
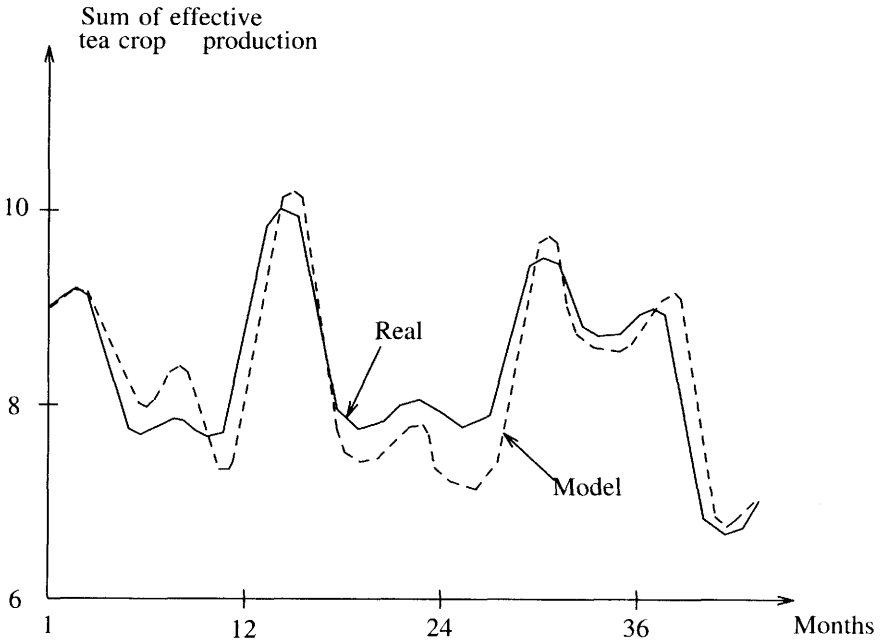
Figure 4.15. Performance of the harmonic model with $L = 4$

so on. These perturbations are estimated by several indices, such as the K- and A-indices and the geomagnetic field components H, F, D, etc.

Here the scope of the example is limited to the use of first formulation to compare the performances of individual models and system of equations. The combinatorial inductive algorithm is used in synthesizing the models.

Experiment 1. Because MAF variations depend on the time of the day, time of day is considered one of the arguments. The following complete polynomial is considered in the first experiment.

$$q^t = a_0 + a_1 t_t + a_2 q^{t-1} + a_3 q_{t-2} + \cdots + a_k q^{t-\tau}$$
$$+ a_{k+1} q^{t-1} t^{t-1} + a_{k+2} q^{t-2} t^{t-2} + \cdots + a_{2k} q_{t-\tau} t^{t-\tau}, \tag{4.88}$$

where $t^t, t^{t-1}, \cdots, t^{t-\tau}$ are the time values corresponding to the output variable and its delayed arguments.

Observations are made for five days and 65 data points were tabulated. Two series of data are made up: one for interval of small variations (from 8AM to 8PM), another for interval of sharp variations (from 8PM to 8AM). For these two types intervals of data, individual models are constructed considering $\tau = 5$. The prediction criterion i is used to select these models; for an interval of small MAF variation

$$q^t = 18.13 + 0.0229 q^{t-3} t^{t-3} - 0.0183 q^{t-5} t^{t-5}. \tag{4.89}$$

For an interval of sharp MAF variation

$$q^t = 10.26 + 0.6554 t^t + 0.3299 q^{t-1} + 0.1109 q^{t-2} - 0.1802 q^{t-5}$$
$$+ 0.0013 q^{t-1} t^{t-1} - 0.0078 q^{t-2} t^{t-2} + 0.0106 q^{t-3} t^{t-3}$$
$$- 0.0138 q^{t-4} t^{t-4} + 0.0152 q^{t-5} t^{t-5}. \tag{4.90}$$

In addition to the above, another model is constructed without having to divide the data into separate segments.

$$q^t = 8.55 + 0.0413t^t + 0.359q^{t-1} + 0.0289q^{t-2} + 0.2283q^{t-3} - 0.0351q^{t-4}$$
$$0.0032q^{t-1}t^{t-1} + 0.0066q^{t-5}t^{t-5}. \tag{4.91}$$

Figure 4.16a demonstrates the performance of predictions of these models. The thin line indicates the actual MAF variations for 12 hours ahead, the thick line is for predictions using two individual models, and the broken line is the predictions using the single model. Two individual models are considerably more accurate in comparison to the single model.

Experiment 2. Here two-dimensional readout (t, T) is used—t indicates the time in hours and T indicates the time in days. The value of the process output variable q is taken as the average for each hour. The complete polynomial is considered as:

$$q_{t,T} = f_t(q_{t-1,T}, q_{t-2,T}, \cdots, q_{t-\tau_t,T}, q_{t,T-1}, q_{t,T-2}, \cdots,$$
$$q_{t,T-\tau_T}, \sigma_{2_{t-1,T}}, \sigma_{3_{t-1,T}}, \cdots, \sigma_{L_{t-1,T}}), \tag{4.92}$$

where $t = 1, \cdots, 24$; τ_t and τ_T are the limits of the delayed arguments on both directions t and T, correspondingly. $\sigma_{k_{t-1,T}}, k = 2, 3, \cdots, L$ are the moving averages, maximum length of L considered.

   Combinatorial algorithm is used to select the F variants of 24 models in relation to the combined criterion of "minimum bias plus regularity." From these F variants of 24 hourly models, one model—the best set of 24 models—is chosen according to the prediction balance criterion,

$$B_{day}^2 = \sum_{j=1}^{N}(\bar{q}_j - \frac{1}{24}\sum_{i=1}^{24}\hat{q}_{i,j})^2, \tag{4.93}$$

where $\bar{q}_j, j$- 1, 2, $\cdots, N$ are the daily averages of MAF variations for N days; $\hat{q}_{i,j}, i = 1, 2, \cdots, 24$, $j = 1, 2, \cdots, N$ are the estimated values of the hourly values using the hourly models by step-by-step predictions given the initial values. The hourly data was collected for 25 days and arranged in two-dimensional readout. The system of equations obtained are

$$q_{1,T} = -0.298 + 0.45q_{24,T} + 0.459\sigma_{6_{24,T}},$$
$$q_{2,T} = 0.497 + 0.892q_{1,T},$$
$$q_{3,T} = 1.929 + 0.8q_{2,T},$$
$$q_{4,T} = -0.208 + 0.289q_{3,T} - 0.399q_{2,T} + \sigma_{3_{3,T}},$$
$$q_{5,T} = 2.006 + 1.715q_{4,T} - 0.979q_{3,T} - 2.052\sigma_{3_{4,T}} + 0.199\sigma_{6_{4,T}},$$
$$q_{6,T} = 3.13 + 0.814q_{5,T} - 0.057q_{6,T-1},$$
$$q_{7,T} = 2.58 + 0.619q_{6,T} - 0.263q_{5,T},$$
$$q_{8,T} = 1.51 + 0.072q_{8,T-1} + 1.11\sigma_{3_{7,T}},$$
$$q_{9,T} = -0.607 - 0.308q_{8,T} + 1.644q_{7,T} + 0.636\sigma_{3_{8,T}} - 0.773\sigma_{6_{8,T}},$$
$$q_{10,T} = 3.596 + 0.788q_{9,T},$$
$$q_{11,T} = 0.816 + 1.084q_{10,T} - 0.156q_{11,T-1},$$
$$q_{12,T} = 3.54 - 0.309q_{12,T-1} + 1.107\sigma_{3_{11,T}},$$
$$q_{13,T} = -0.857 + 1.089\sigma_{3_{12,T}},$$
$$q_{14,T} = -0.824 + 0.069q_{14,T-1} + 2.584\sigma_{3_{13,T}} - 1.576\sigma_{6_{13,T}},$$
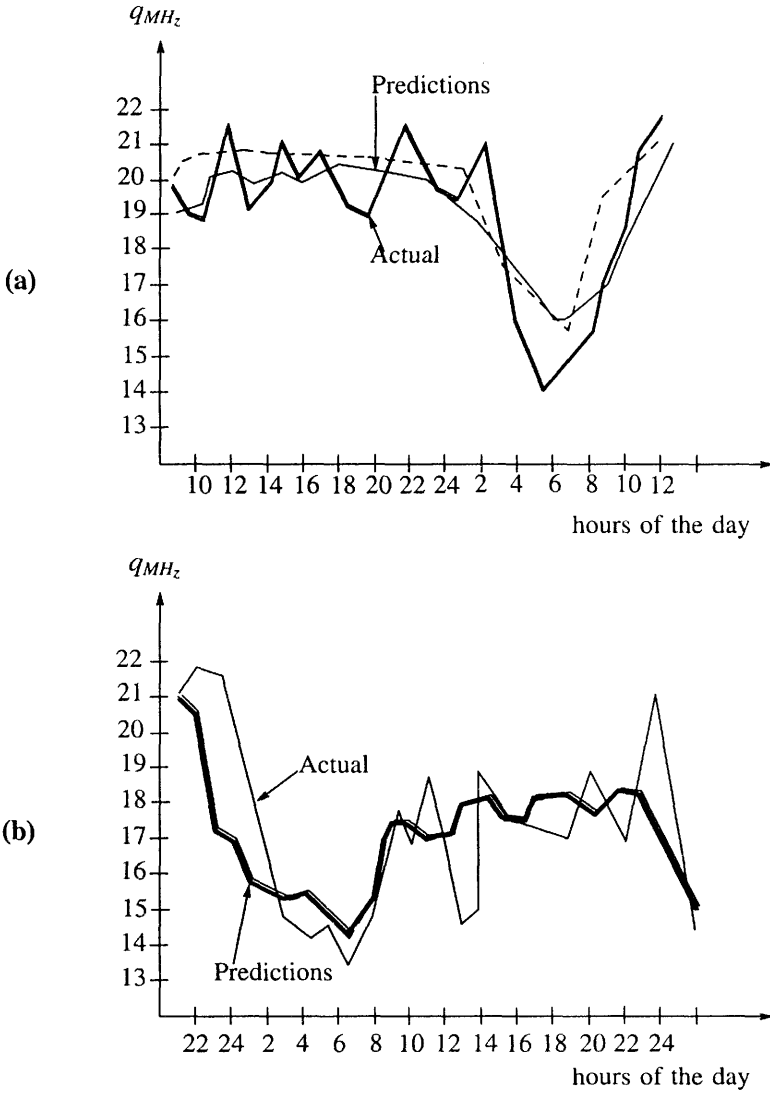
Figure 4.16. (a) Predictions using individual models and (b) predictions using system of equations

$$q_{15,T} = 5.12 + 0.8q_{14,T} - 0.107q_{15,T-1},$$

$$q_{16,T} = 5.104 + 0.806q_{15,T} - 0.988\sigma_{3_{15,T}} + 0.887\sigma_{6_{15,T}},$$

$$q_{17,T} = 0.822 + 1.151q_{16,T} - 0.058q_{17,T-1} + 0.493\sigma_{3_{16,T}} - 0.598\sigma_{6_{16,T}},$$

$$q_{18,T} = 2.976 + 1.172\sigma_{3_{17,T}} - 0.311\sigma_{6_{17,T}},$$

$$q_{19,T} = -9.478 + 3.079q_{18,T} + 0.302q_{19,T-1} - 1.908\sigma_{3_{18,T}},$$

$$q_{20,T} = -2.436 + 1.119q_{19,T},$$

$$q_{21,T} = 3.056 + 2.592q_{20,T} + 2.774q_{19,T} - 5.734\sigma_{3_{20,T}} + 1.225\sigma_{6_{20,T}},$$

$$q_{22,T} = -4.317 - 0.727q_{20,T} + 0.023q_{22,T-1} + 1.595\sigma_{3_{21,T}},$$

$$q_{23,T} = 10.57 + 2.316q_{22,T} - 0.85\sigma_{3_{22,T}} - 1.087\sigma_{6_{22,T}},$$

$$q_{24,T} = 1.683 + 0.797\sigma_{3_{23,T}} \tag{4.94}$$

Figure 4.16b exhibits the actual and forecast values of the MAF variations on 24-hour duration of the interval considered. It shows that the models of this class select a basically regular cyclical component in the process.

Inductive algorithms make it possible to synthesize more universal models to forecast both regular and abrupt irregular MAF variations by providing the information on external perturbations. This also makes it possible to raise forecast accuracy and anticipation time by using prediction balance criterion with two-dimensional time readout.